Analysis of time dependent problems using exponential basis functions

B. Movahedian
B. Boroomand

Publication CIMNE Nº-364, July 2011

Analysis of time dependent problems using exponential basis functions

B. Movahedian
B. Boroomand

Publication CIMNE Nº-364, July 2011

International Center for Numerical Methods in Engineering
Gran Capitán s/n, 08034 Barcelona, España

Analysis of Time Dependent Problems Using Exponential Basis Functions

B. Movahedian and B. Boroomand

Department of Civil Engineering, Isfahan University of Technology, Isfahan 84156-83111, Iran

Abstract

In this research we present a method based on using Exponential Basis Functions (EBFs) to solve a class of time dependent engineering problems. The solution is first approximated by a summation of EBFs satisfying the differential equation and then completed by satisfying the time dependent boundary conditions as well as the initial conditions through a collocation method. This can be performed by considering two approaches. In the first one the solution is split into three parts, i.e. a homogeneous solution obtained by homogeneous boundary conditions, a homogeneous solution obtained by non-homogeneous solution and finally a particular solution induced by source terms. In the second approach the solution is split into two parts, i.e. a homogeneous solution and a particular solution induced by source terms. The two approaches are then employed to construct a time marching algorithm for the solution of problems over a long period of time.

We shall present the details of the application of the two approaches introduced to some mathematical and engineering problems. The details of the time marching algorithm proposed are explained. Several problems are solved to show the capabilities of the approaches used. Some benchmark problems are also devised and solved for further studies. It is shown that the one of the introduced approaches is capable of solving a class of problems with moving boundaries.

Keywords: *Time-dependent, Exponential basis functions, Fundamental solution, Collocation, Discrete transformation, Meshless method*

Contents

1. Introduction

After about a century from the development of efficient numerical methods such as Finite difference method (FDM), finite element method (FEM) or boundary element method (BEM), the need of further developments for attaining high accuracy solutions is still felt in some engineering problems. An instance may be seen in wave propagation problems involving high frequency excitation encountering in crack detection procedures. Among the ideas for improving the available routines, one may find studies on using alternative basis in FDM as in [1] or in FEM as [2-4]. Compared with FDM and FEM, BEM is capable of producing solutions with high accuracy. However, the necessity of using elements at the boundaries introduces some undesirable features in many applications. The method of fundamental solutions (MFS) has emerged as an alternative to BEM and so far has proved to be effective in many problems [5, 6]. Both BEM and MFS are sometimes categorized in Trefftz methods. However, these two methods require basis functions which are not available in many problems. Most of the above mentioned methods are basically devised for solution of problems defined in spatial coordinates.

For problems defined in spatial coordinates and time, the methods are sometimes combined with FDM (e.g. Newmark methods [7] or combined with Trefftz method [8]) or they are used in conjunction with a suitable transformation technique such as Fourier or Laplace transformation (see [9-11]). In the latter case, finding the inverse of the solution is another difficult task.

Among the aforementioned numerical methods considering time directly, MFS seems to be more attractive to many researches [12-15], although the list of the studies in this regard is short. Due to the limitation of availability of the fundamental solution, most of the studies focus on heat conduction problems for which the bases are known [13-15]. However, such fundamental solutions are not available for many other cases even in the realm of problems whose governing differential equation is of constant coefficient type. Nevertheless, it is mathematically understood that for this latter type of problems one can always find some bases in the form of exponential functions. This helps to construct a Trefftz method for such a category of problems. As shown in [16], a Trefftz collocation approach is well suited for this purpose.

In this research we extend the idea used in [16, 17] to solve time dependent problems. We shall focus on problems having application in engineering, such as heat conduction or wave propagation ones. Considering time as an axis, we treat the problems in manner similar to that introduced in [16] while acknowledging the fact that in this case the problems are of initial value type. As is seen later, we shall cast the method in two forms of approaches, in one exponential basis functions (EBFs) are used to construct a non-standard eigenvalue problem and another directly EBFs are employed in a manner similar to procedure introduced in [16]. In both approaches we satisfy the non-homogenous boundary conditions through collocation. In some special cases, part of the procedure in the first approach becomes similar to Sturm-Liouville problems [9, 10] and thus results in a set of orthogonal eigen-functions. However, the problems we consider here are of more general forms and thus the eigen-functions are not necessarily orthogonal which makes the satisfaction of the initial boundary conditions more difficult, compare with Sturm-Liouville problems. This effect may be viewed as a convincing reason for using collocation for satisfaction of the initial conditions. A rather similar idea has recently been tested successfully in boundary value problems [18]. In the second approach we satisfy the initial and side conditions at the same time through collocation.

As will be seen later, a finite time interval is predefined in the method presented and this effect resembles other methods using MFS. However, in many practical problems it is needed to consider a rather long period of time for simulation. We shall introduce a time marching procedure with the aid of the two proposed approaches. To this end, we choose a small time interval and repeat the procedure in a step by step manner while using the information obtained at the end of time interval as the initial values for the next step. We shall show that such an algorithm affects the accuracy of the solution.

The idea of treating time as an axis similar to those used for special coordinates appears to be rather new. Few studies have focused on such an idea most of which use the method of fundamental solutions (MFS) in a certain class of problems [12-15]. This makes it hard to find benchmarks especially when a wider class of problems is of interest. Most of the benchmarks may be found in references addressing classical mathematics where separation of variables is used to solve the time dependent problem through some well-known transformation techniques [9, 10].

The method is to be tested in solution of well-known engineering problems. Heat conduction and wave propagation problems are chosen for this purpose. Some of the problems defined are solvable through well-known approaches such as using Fourier series [9, 10]. We shall use such solutions as the reference ones for those particular benchmark problems. However, as will be seen later, there are some engineering problems, in the two aforementioned categories, which are not easily solvable with the standard approaches. We shall show that the introduced collocation method is capable of solving many of such problems. In the same line, we shall show how more general mathematical problems can be solved using the proposed method.

The layout of the report is as follows. In the next section the model used in this research is described. In Section 3 we address the way that the EBFs are found. In Section 5 the solution method is described where we introduce two approaches for our method.

Formulation suitable for the solution of problems with source terms is explained in the same section. In Section 5 we shall introduce the time marching algorithm mentioned earlier. In the next section we shall consider two sample problems as general mathematical ones. The problems are defined so that the well-known approaches can not easily be applied. Also in section 7 we shall consider five more sample problems in the category of engineering problems some of which may not be solved with standard mathematical methods. In the same section we shall show how the approach II may be used to solve a class of problems with moving boundaries. Finally in Section 8 we shall summarize the conclusions made throughout the research.

2. Model problems

We consider a general 1D time dependent problem with following equation

$$\sum_{n=0}^{N} a_n \frac{\partial^n u}{\partial x^n} + \sum_{m=1}^{M} b_m \frac{\partial^m u}{\partial t^m} + \sum_{n=1}^{N}\sum_{m=1}^{M} a_{nm} \frac{\partial^{n+m} u}{\partial x^n \partial t^m} = q(x,t) \quad x_L \le x \le x_R \,,\ t \ge 0 \tag{1}$$

In the above equation u is the main unknown function to be found in spatial coordinate x and time t, a_n, b_m and a_{nm} are the representatives of three sets of constant coefficients (with at least one non-zero element in each set of every two chosen sets for $n \ge 1$ and $m \ge 1$, respectively), N and M are the maximum orders of differentiation with respect to x any t, and finally q is a predefined source term varying with x and t. The following generalized end boundary conditions are also defined

$$\sum_{k=0}^{K_L^i} \overline{c}_{i,k} \left[\frac{\partial^k u}{\partial x^k} \right]_{x=x_L} = L_i(t) \,, \qquad i = 1,....,N_1 \,, \tag{2}$$

$$\sum_{k=0}^{K_R^j} \overline{d}_{j,k} \left[\frac{\partial^k u}{\partial x^k} \right]_{x=x_R} = R_j(t) \,, \qquad j = 1,....,N_2 \,, \tag{3}$$

Here again $\overline{c}_{i,k}$ and $\overline{d}_{j,k}$ are the representatives of $N_1 + N_2$ sets of constant coefficients (with at least one non-zero element in each set). K_L^i and K_R^j are the maximum order of derivatives appearing in the end conditions at x_L and x_R, respectively (in many practical problems

$K_L^i \le N$ and $K_R^j \le N$). Also $L_i(t)$ and $R_j(t)$ represent two sets of time dependent functions defined at $x = x_L$ and $x = x_R$.

The reader may note that for a solvable problem with definition (1), each set of the relations in (2) and (3) should give, respectively, N_1 and N_2 distinct but not over-determined conditions. Besides, the total number of conditions at both sides should satisfy $N_1 + N_2 = N$.

The initial boundary conditions may generally be expressed as follows

$$\sum_{k=0}^{I^P} \bar{e}_{P,k} \left[\frac{\partial^k u}{\partial t^k} \right]_{t=0} = F_P(x), \qquad P = 1,....,M \ , \quad x_L \le x \le x_R \tag{4}$$

where $\bar{e}_{P,k}$ represents M sets of coefficients (with at least one non-zero element in each set). $F_P(x)$ is an element of a set of functions defined in spatial coordinate as initial values. The maximum order of differentiation I^P in each set, for engineering problems, is usually equal or less than M (here again the relations (4) should be a set of M distinct but not over-determined conditions).

In the above relations the left and right ends of the problem are considered fixed, however for problems with moving boundaries one may consider the end coordinates as functions of time, i.e. $x_L(t)$ and $x_R(t)$. We shall give some examples in the part of numerical results.

3. Exponential Basis Functions

The solution to the problem defined in (1) may be split into homogeneous and particular parts as

$$u = u_H + u_P \tag{5}$$

where u_H is the solution to (1) with $q = 0$ and u_P is the solution when $q \ne 0$ disregarding the boundary conditions. Generally the summation may contain smooth and non-smooth parts. Here we focus on the smooth solutions so that they can be expressed as the summation of some exponential functions. For homogeneous part, for instance, the following exponential form is considered

$$u_H(x,t,\alpha,\beta) = A(\alpha,\beta)e^{\alpha x + \beta t} \tag{6}$$

Substitution of (6) in (1), with $q = 0$, results in a relation which is satisfied when the following algebraic equation holds

$$\sum_{n=0}^{N} a_n \alpha^n + \sum_{m=1}^{M} b_m \beta^m + \sum_{n=1}^{N} \sum_{m=1}^{M} a_{nm} \alpha^n \beta^m = 0 \tag{7}$$

From the above equation either of the parameters α or β may be found in terms of another

$$\alpha_n = f_n(\beta) \qquad n = 1,.....,N \tag{8}$$

or

$$\beta_m = \bar{f}_m(\alpha) \qquad m = 1,.....,M \tag{9}$$

This may be performed either explicitly by finding the functions or numerically by choosing one and calculating the roots of the algebraic equation (7).

Remark 1: In some problems the characteristic equation (7) yields multiple roots for α or β. In that case, some of the bases will be missing. The missing bases may be found by considering a polynomial, containing monomials of x and t, multiplied by the original basis. For instance if two repeating roots exist then one may consider $(a+bx+ct)e^{\alpha x+\beta t}$ as a new form of basis (see [16] for similar situation in problems just defined in spatial coordinates). We shall present an example in Section 6 of the report. ■

It must be noted that α and β in (8) and (9) may take on complex values. Therefore, the solution to (1) may be written as

$$u_H = \int_{\Omega_\beta} \sum_{n=1}^{N} A_n(\alpha_n, \beta) e^{\alpha_n x+\beta t} d\Omega_\beta \tag{10}$$

for instance when α is found in terms of β as in (8). In the above relation Ω_β is an appropriate area or locus in the Gaussian plane. The unknown coefficients $A_n(\alpha_n, \beta)$ are to be found so that boundary conditions (2) to (4) are satisfied. This, if not possible, is very difficult task for most problems. However, one may think of a discrete form of (10), for instance when the integral is to be calculated numerically, and simply write

$$\hat{u}_H(x,t) = \sum_{i_0=1}^{N_\beta} \sum_{n=1}^{N} C_{i_0,n} e^{\alpha_{i_0,n} x+\beta_{i_0} t} \qquad \alpha_{i_0,n} = f_n(\beta_{i_0}) \tag{11}$$

In the above equation $\hat{u}_H$ is an approximation to u_H, $C_{i_0,n}$ represents a set of coefficients to be found from boundary conditions, $\alpha_{i_0,n}$ is evaluated by the n th functions in (8) when β_{i_0} is chosen on the Gaussian point, and N_β is the total number of points used in Gaussian plane for β. A similar expression may be written when β is found in terms of α as in (9), thus the approximated function $\hat{u}_H$ may be considered as

$$\hat{u}_H(x,t) = \sum_{i_0=1}^{N_\beta} \sum_{n=1}^{N} C_{i_0,n} e^{\alpha_{i_0,n} x+\beta_{i_0} t} + \sum_{i_0=1}^{N_\alpha} \sum_{m=1}^{M} C_{i_0,m} e^{\alpha_{i_0} x+\beta_{i_0,m} t} \tag{12}$$

with $C_{i_0,m}$, $\beta_{i_0,m}$ and N_α being analogously defined as their counterparts in (11). Instead of working with the forms given above, for convenience, we summarize the expressions as the following one

$$\hat{u}_H(x,t) = \sum_{j_0=1}^{N_e} C_{j_0} e^{\alpha_{j_0} x + \beta_{j_0} t} \tag{13}$$

where N_e is the number of EBFs used. Whenever needed, we shall specify whether α is to be found in terms of β or vice versa. Next we shall explain how one can find the coefficients from the information at the boundaries.

4. The solution method

In this part first we consider problems with no source term, i.e. $q = 0$, and try to satisfy the boundary conditions to obtain a solution for a homogeneous partial differential equation. Having introduced the approaches, we explain how one can deal with problems with source terms.

4.1. Problems without source terms

The aim here is to find appropriate coefficients C_{i_0} in (13) so that the boundary conditions (2) - (4) are fully or approximately satisfied. Two approaches are proposed here in this regard. In the first one we split the solution into two parts through defining a suitable characteristic problem and use two separate collocation schemes. In the second one we directly use a collocation scheme for all boundary conditions. The later approach enables us to solve some class of problems with moving boundaries.

Approach I

We spilt the homogeneous solution into two parts

$$\hat{u}_H = \hat{u}_H^0 + \hat{u}_H^g \tag{14}$$

In the above relation $\hat{u}_H^0$ denote a solution in which side boundary conditions (2) and (3) are considered in their homogeneous forms

$$\sum_{k=0}^{K_L^i} \bar{c}_{i,k} \left[\frac{\partial^k \hat{u}_H^0}{\partial x^k} \right]_{x=x_L} = 0\,, \qquad i = 1, \ldots., N_1 \tag{15}$$

and

$$\sum_{k=0}^{K_R^j} \bar{d}_{j,k} \left[\frac{\partial^k \hat{u}_H^0}{\partial x^k} \right]_{x=x_R} = 0\,, \qquad j = 1,....,N_2 \tag{16}$$

By defining $\hat{u}_H^0$, obviously, the task of satisfying the actual conditions remains for $\hat{u}_H^g$ (this will be explained later). From the two forms in the right hand side of (12) we choose the first one for $\hat{u}_H^0$ and write

$$(\hat{u}_H^0)_\beta = \sum_{n=1}^{N} C_n e^{f_n(\beta)x+\beta t} \tag{17}$$

while we let β to be determined later. Inserting (17) in (16) and (15) results in a characteristic problem

$$\mathbf{A}_\beta \mathbf{C} = \mathbf{0} \tag{18}$$

where $\mathbf{A}_\beta$ is a $N \times N$ matrix depending on β and $\mathbf{C}$ is an $N \times 1$ array containing the coefficients C_n. The elements of $\mathbf{A}_\beta$ are as

$$(\mathbf{A}_\beta)_{n_1,n_2} = \sum_{k=0}^{K_L^{n_1}} \bar{c}_{n_1,k} \left[f_{n_2}(\beta) \right]^k e^{f_{n_2}(\beta)x_L} \qquad n_1 \le N_1\,, \qquad 1 \le n_2 \le N \tag{19}$$

$$(\mathbf{A}_\beta)_{n_1,n_2} = \sum_{k=0}^{K_R^{n_1}} \bar{d}_{n_1,k} \left[f_{n_2}(\beta) \right]^k e^{f_{n_2}(\beta)x_R} \qquad N_1 < n_1 \le N\,, \quad 1 \le n_2 \le N \tag{20}$$

For non-trivial solution of (18), the determinant of $\mathbf{A}_\beta$ is set zero

$$|\mathbf{A}_\beta| = 0 \tag{21}$$

This is a non-standard eigenvalue problems which should be solved for β. One may arrange the values in terms of their Hermitian length $|\beta|$ and thus use a counter as "l" to distinguish the eigenvalues and eigenvectors as

$$\beta_l = s_l\,, \quad \mathbf{C}_l = \boldsymbol{\phi}_l \qquad l \in \mathbb{N} \tag{22}$$

The first part of the homogeneous solution is therefore written as

$$\hat{u}_H^0 = \sum_l c_l \left(\sum_{n=1}^{N} (\phi_l)_n e^{f_n(s_l)x+s_l t} \right) \tag{23}$$

In (23) c_l denotes a set of new unknown coefficients to be determined from non-zero boundary conditions and $(\phi_l)_n$ is the nth element of $\boldsymbol{\phi}_l$.

Remark 2: The characteristic problem defined above has much in common with Sturm-Liouville problems; however the elements of the series (23) are not necessarily orthogonal in all cases. Nevertheless the problem may be reduced to a Sturm-Liouville when the operators in (1) and boundary conditions (2) and (3) are arranged in an appropriate form [9, 10]. We shall refer to this effect in the Section 7 of the report where the engineering problems are dealt with. ■

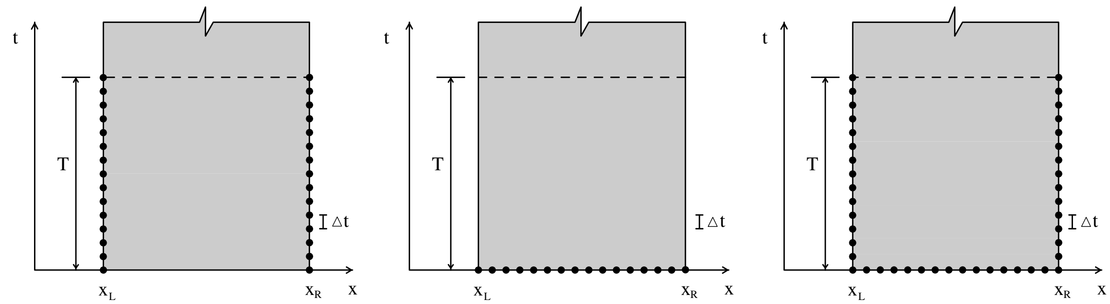

(a) (b) (c)

Figure 1. Schematic presentation of the solution domain; the points used for satisfaction of (a) the side boundary conditions in approach I, (b) the initial conditions in approach I, (c) the side and initial conditions in approach II.

The second part of the homogeneous solution $\hat{u}_H^g$ may be constructed by an expression similar to (17) but with parameter β different from those obtained as (22). To this end we choose a set of values for β as

$$\beta_r = w_r \qquad w_r \notin \{s_l, l \in \mathbb{N}\} \tag{24}$$

Prior to construction of $\hat{u}_H^g$, one should express the right hand sides of (2) and (3) in terms of exponential functions in time; i.e.

$$L_i(t) = \sum_{r=1}^{N_e^t} (h_L)_{i,r} e^{w_r t}\ , \qquad i = 1,....,N_1 \tag{25}$$

and

$$R_j(t) = \sum_{r=1}^{N_e^t} (h_R)_{j,r} e^{w_r t}\ , \qquad j = 1,....,N_2 \tag{26}$$

In the above relations $(h_L)_{i,r}$ and $(h_R)_{j,r}$ are two sets of new coefficients to be determined from $L_i(t)$ and $R_j(t)$. Also N_e^t is the number of exponential functions to be used. Note that exponential functions $e^{w_r t}$ are not necessarily orthogonal. To find $(h_L)_{i,r}$ and $(h_R)_{j,r}$ we employ a collocation scheme. First of all we consider a finite interval of time as $t \in [0,T]$ instead of $t \in [0,\infty)$. The largeness of T may be determined by inspection, i.e. in a successive solutions one can enlarge T until the final approximation to u converges to a solution for smaller time interval $t \in [0, T_1]$, $T_1 < T$. We then sample $L_i(t)$, $R_j(t)$ and $e^{w_r t}$ at N_p^t points along t (see Figure 1-a)

$$\mathbf{L}_i = \left[L_i(t_1) \quad L_i(t_2) \quad ...... \quad L_i(t_{N_p^t}) \right]^T$$
$$\mathbf{R}_j = \left[R_j(t_1) \quad R_j(t_2) \quad ...... \quad R_j(t_{N_p^t}) \right]^T \tag{27}$$
$$\mathbf{e}_r = \left[e^{w_r t_1} \quad e^{w_r t_2} \quad ..... \quad e^{w_r t_{N_p^t}} \right]^T$$

and rewrite (25) and (26) in their discrete form

$$\mathbf{L}_i = \sum_{r=1}^{N_e^t} (h_L)_{i,r} \mathbf{e}_r , \quad \mathbf{R}_j = \sum_{r=1}^{N_e^t} (h_R)_{j,r} \mathbf{e}_r \tag{28}$$

Note that the number of sampling points should not necessary be equal (or even greater than) the number of bases. The coefficients $(h_L)_{i,r}$ and $(h_R)_{j,r}$ can simply be found as

$$(h_L)_{i,r} = \mathbf{e}_r^T \mathbf{r} \, \mathbf{L}_i , \quad (h_R)_{j,r} = \mathbf{e}_r^T \mathbf{r} \, \mathbf{R}_j \tag{29}$$

where $\mathbf{r}$ is a $N_p^t \times N_p^t$ projection matrix which can be evaluated (see [16-21]) by inserting relations (28) in (29) as

$$\mathbf{r} = \left[\sum_{r=1}^{N_p^t} \mathbf{e}_r \mathbf{e}_r^T \right]^+ \tag{30}$$

In the above equation $[.]^+$ denotes the pseudo-inverse of the matrix. Note that in (28) to (30) normalized arrays as $\overline{\mathbf{e}}_r = \frac{1}{a} \mathbf{e}_r$, with a being an appropriate scaling factor, may be used (see [16]).

Remark 3: The reader may note that in choosing w_r the point spacing used for the sampling plays an important role. Here we choose w_r so that oscillation of the function $e^{w_r t}$ happens within a period greater than $4\Delta t$, with Δt being the spacing between the points along t axes. This leads us to consider a restriction for the imaginary part of w_r as $\left| \Im(w_r) \right| \le \frac{\pi}{2\Delta t}$. ■

Remark 4: In the evaluation of $(h_L)_{i,r}$ and $(h_R)_{j,r}$ one may use the extended forms of the side conditions, i.e. $L_i(t)$ and $R_j(t)$ may be fictitiously extended to $t < 0$. This helps to construct a smooth $\hat{u}_H^g$ so that the initial boundary conditions are satisfied effectively. ■

With $(h_L)_{i,r}$ and $(h_R)_{j,r}$ in hand, a new system of equations similar to (18) but with non-zero right hand side are arranged as

$$\mathbf{A}_{w_r}\mathbf{C}_r = \mathbf{h}_r\,, \qquad r = 1,....,N_e^t \tag{31}$$

In (31) $\mathbf{C}_r = \left[C_{r,1} \quad ... \quad C_{r,N} \right]$ is a set of N coefficients and

$$\mathbf{h}_r = [\underbrace{... \quad (h_L)_{i,r} \quad ...}_{N_1} | \underbrace{... \quad (h_R)_{j,r} \quad ....}_{N_2}]^T \tag{32}$$

The elements of $\mathbf{A}_{w_r}$ are as

$$(\mathbf{A}_{w_r})_{n_1,n_2} = \sum_{k=0}^{K_L^{n_1}} \overline{c}_{n_1,k} \left[f_{n_2}(w_r) \right]^k e^{f_{n_2}(w_r)x_L} \qquad n_1 \le N_1\,, \qquad 1 \le n_2 \le N \tag{33}$$

$$(\mathbf{A}_{w_r})_{n_1,n_2} = \sum_{k=0}^{K_R^{n_1}} \overline{d}_{n_1,k} \left[f_{n_2}(w_r) \right]^k e^{f_{n_2}(w_r)x_R} \qquad N_1 < n_1 \le N\,, \quad 1 \le n_2 \le N \tag{34}$$

Since $\mathbf{A}_{w_r}$ is regular, one may find the coefficients of $\mathbf{C}_r$ as

$$\mathbf{C}_r = \mathbf{A}_{w_r}^{-1}\mathbf{h}_r \tag{35}$$

The second part of the homogeneous solution is therefore written as

$$\hat{u}_H^g = \sum_{r=1}^{N_e^t} \left(\sum_{n=1}^{N} C_{r,n} e^{f_n(w_r)x + w_r t} \right) \tag{36}$$

In view of (23) and (36) the complete form of the homogeneous solution is now written as

$$\hat{u}_H = \sum_l c_l \left(\sum_{n=1}^{N} (\phi_l)_n e^{f_n(s_l)x + s_l t} \right) + \sum_{r=1}^{N_e^t} \left(\sum_{n=1}^{N} C_{r,n} e^{f_n(w_r)x + w_r t} \right) \tag{37}$$

Remark 5: In view of Equations (25) and (26), it may be seen that Fourier series may also be used to express $L_i(t)$ and $R_j(t)$. In that case one may write

$$L_i(t) = \sum_{r=-\infty}^{\infty} (\overline{h}_L)_{i,r} e^{2\mathbf{i}r\pi t/T}\,, \qquad (\overline{h}_L)_{i,r} = \frac{1}{T}\int_{-T}^{T} L_i(t) e^{-2\mathbf{i}r\pi t/T} dt \tag{38}$$

$$R_j(t) = \sum_{r=-\infty}^{\infty} (\overline{h}_R)_{j,r} e^{2\mathbf{i}r\pi t/T}\,, \qquad (\overline{h}_R)_{j,r} = \frac{1}{T}\int_{-T}^{T} R_j(t) e^{-2\mathbf{i}r\pi t/T} dt \tag{39}$$

Upon selecting a finite number for r in this case, e.g. $-N_r \le r \le N_r$, the right hand side of (31) is replaced by the following array

$$\overline{\mathbf{h}}_r = [\underbrace{... \quad (\overline{h}_L)_{i,r} \quad ...}_{N_1} | \underbrace{... \quad (\overline{h}_R)_{j,r} \quad ....}_{N_2}]^T \tag{40}$$

The elements of $\mathbf{A}_{w_r}$ will be as those given in (33) and (34) with w_r replaced by $\mathbf{i}r\pi/T$. The rest of the procedure will be as explained before (see relations (35)-(37)). Note that in this case, one should extend the side conditions to $t<0$ (see Remark 4). We shall present the results of such a formulation in the sample problem 5. ■

The remaining unknowns in (37) are the coefficients c_l which are to be found from the initial conditions (4). Note that the number of these unknown coefficients may be increased by finding new s_l from the characteristic equation (21).

In order to find the coefficients c_l first we substitute (37) in (4) as

$$\sum_{k=0}^{I^P} \overline{e}_{P,k} \left[\frac{\partial^k \hat{u}_H}{\partial t^k} \right]_{t=0} = F_P(x)\,, \qquad P=1,....,M \tag{41}$$

which leads to

$$\sum_{k=0}^{I^P} \overline{e}_{P,k} \left\{ \sum_l c_l s_l^k \left(\sum_{n=1}^{N} (\phi_l)_n e^{f_n(s_l)x} \right) + \sum_{r=1}^{N_e^t} w_r^k \left(\sum_{n=1}^{N} C_{r,n} e^{f_n(w_r)x} \right) \right\} = F_P(x) \tag{42}$$

By rearranging the summation signs, one may write

$$\sum_l c_l B_{P,l}(x) + \overline{F}_{P,l}(x) = F_P(x)\,, \quad P=1,....,M \tag{43}$$

where

$$B_{P,l}(x) = \sum_{k=0}^{I^L} \overline{e}_{P,k} s_l^k \left(\sum_{n=1}^{N} (\phi_l)_n e^{f_n(s_l)x} \right), \qquad \overline{F}^P(x) = \sum_{k=0}^{I^l} \overline{e}_{P,k} \sum_{r=1}^{N_e^t} w_r^k \left(\sum_{n=1}^{N} C_{r,n} e^{f_n(w_r)x} \right) \tag{44}$$

Once again, we employ a collocation scheme to find c_l in (43). To this end, a number of sampling points, say N_p^x , are chosen along $x_L \le x \le x_R$ at $t=0$ (see Figure 1-b). Then the functions at both sides of (43) are calculate at the points to obtain

$$\sum_l c_l \mathbf{B}_{P,l} + \overline{\mathbf{F}}_P = \mathbf{F}_P \qquad\qquad P=1,....,M \tag{45}$$

We further arrange all conditions as

$$\sum_l c_l \widehat{\mathbf{B}}_l + \widehat{\overline{\mathbf{F}}} = \widehat{\mathbf{F}} \tag{46}$$

For instance $\widehat{\mathbf{F}}$ is an $(M.N_p^x)\times 1$ array arranged as follows

$$\widehat{\mathbf{F}} = \left[(\mathbf{F}_1)^T\, (\mathbf{F}_2)^T \quad .. \quad (\mathbf{F}_P)^T \quad .. \quad (\mathbf{F}_M)^T \right]^T, \quad (\mathbf{F}_P)^T = \left[F_P(x_1) \quad F_P(x_2) \quad ..... \quad F_P(x_{N_p^x}) \right] \tag{47}$$

The coefficients c_l are found as

$$c_l = \overline{\mathbf{B}}_l^T \overline{\mathbf{R}}\,(\overline{\mathbf{F}} - \hat{\overline{\mathbf{F}}}) , \qquad \overline{\mathbf{R}} = \left[\sum_l \overline{\mathbf{B}}_l \overline{\mathbf{B}}_l^T \right]^+ \tag{48}$$

The final solution is then obtained as

$$\hat{u}_H = \left[\sum_l \left(\sum_{n=1}^{N} (\phi_l)_n e^{f_n(s_l)x + s_l t} \right) \overline{\mathbf{B}}_l^T \right] \overline{\mathbf{R}}\,(\overline{\mathbf{F}} - \hat{\overline{\mathbf{F}}}) + \sum_{r=1}^{N_e^t} \left(\sum_{n=1}^{N} C_{r,n} e^{f_n(w_r)x + w_r t} \right) \tag{49}$$

Here again one may also use a normalized form of the arrays $\overline{\mathbf{B}}_l$ (see [16]).

Remark 6: It may be noted that the point spacing along x axes must be selected by considering the fluctuation of the function $e^{f_n(s_l)x}$. By restricting the oscillation of the function within a period greater than $4\Delta x$, with Δx being the spacing, one may find a relation between the point spacing and the imaginary part of $f_n(s_l)$ as $2\Delta x \times \max \left| \Im(f_n(s_l)) \right| \le \pi$. This means that the larger N the smaller point spacing Δx. ■

The above approach may be followed for many engineering problems. We shall explain the procedure for some well-known problems. But before that, next we shall propose another approach without splitting the homogeneous part of the solution.

Approach II

In this approach we directly use Equation (13) and try to find the coefficients C_i by a collocation scheme for boundary conditions (2), (3) and (4) simultaneously. Unlike the first approach the relations (8) and (9) are both used in this case. To this end we substitute (13) in the boundary conditions which leads to the following sets of equations

$$\sum_{j_0=1}^{N_e} C_{j_0} \sum_{k=0}^{K_L^i} \overline{c}_{i,k}\, \alpha_{j_0}^k\, e^{\alpha_{j_0} x_L + \beta_{j_0} t} = L_i(t) , \qquad i = 1, ..., N_1 \tag{50}$$

for the left conditions at $x = x_L$ and

$$\sum_{j_0=1}^{N_e} C_{j_0} \sum_{k=0}^{K_R^j} \overline{d}_{j,k}\, \alpha_{j_0}^k\, e^{\alpha_{j_0} x_R + \beta_{j_0} t} = R_j(t) , \qquad j = 1, ..., N_2 \tag{51}$$

for the right conditions at $x = x_R$ and finally

$$\sum_{j_0=1}^{N_e} C_{j_0} \sum_{k=0}^{I^P} \overline{e}_{P,k}\, \beta_{j_0}^k\, e^{\alpha_{j_0} x} = F_P(x) , \qquad P = 1, ..., M \tag{52}$$

for the initial conditions at $t=0$. Here again we sample both sides of (50) and (51) at N_p^t points along t and at the same time sample both sides of (52) at N_p^x points to write

$$\sum_{j_0=1}^{N_e} C_{j_0} (\mathbf{e}_{j_0}^L)_i = \mathbf{L}_i \qquad i=1,....,N_1 \tag{53}$$

as the collocated values at $x=x_L$ and

$$\sum_{j_0=1}^{N_e} C_{j_0} (\mathbf{e}_{j_0}^R)_j = \mathbf{R}_j \qquad j=1,....,N_2 \tag{54}$$

as the collocated values at $x=x_R$ and

$$\sum_{j_0=1}^{N_e} C_{j_0} (\mathbf{f}_{j_0})_P = \widehat{\mathbf{F}}_P, \qquad P=1,....,M \tag{55}$$

as the collocated values at $t=0$ (see Figure 1-c). The definitions of $\mathbf{L}_i$ and $\mathbf{R}_j$ are the same as those given in (27) and that of the $\widehat{\mathbf{F}}_P$ is the same as the second relation in (47). The definitions of $(\mathbf{e}_{j_0}^L)_i$, $(\mathbf{e}_{j_0}^R)_j$ and $(\mathbf{f}_{j_0})_P$ are, respectively, as

$$(\mathbf{e}_{j_0}^L)_i = \left[\sum_{k=0}^{K_R^j} \bar{d}_{j,k}\, \alpha_{j_0}^k\, e^{\alpha_{j_0} x_L + \beta_{j_0}(t_1)}, \quad .... \quad , \sum_{k=0}^{K_R^j} \bar{d}_{j,k}\, \alpha_{j_0}^k\, e^{\alpha_{j_0} x_L + \beta_{j_0}(t_{N_p^t})} \right]^T \tag{56}$$

$$(\mathbf{e}_{j_0}^R)_j = \left[\sum_{k=0}^{K_R^j} \bar{d}_{j,k}\, \alpha_{j_0}^k\, e^{\alpha_{j_0} x_R + \beta_{j_0}(t_1)}, \quad .... \quad , \sum_{k=0}^{K_R^j} \bar{d}_{j,k}\, \alpha_{j_0}^k\, e^{\alpha_{j_0} x_R + \beta_{j_0}(t_{N_p^t})} \right]^T \tag{57}$$

$$(\mathbf{f}_{j_0})_P = \left[\sum_{k=0}^{I^P} \bar{e}_{P,k}\, \beta_{j_0}^k\, e^{\alpha_{j_0}(x_1)}, \quad .... \quad , \sum_{k=0}^{I^P} \bar{e}_{P,k}\, \beta_{j_0}^k\, e^{\alpha_{j_0}(x_{N_p^x})} \right]^T \tag{58}$$

A new arrangement of equations (53), (54) and (55), for all i, j and P, may be rewritten as

$$\sum_{j_0=1}^{N_e} C_{j_0} \mathbf{V}_{j_0} = \mathbf{U}, \tag{59}$$

where

$$\mathbf{V}_{j_0} = [\underbrace{(\mathbf{e}_{j_0}^L)_1^T ......(\mathbf{e}_{j_0}^L)_{N_1}^T}_{for\ i=1,....,N_1} \mid \underbrace{(\mathbf{e}_{j_0}^R)_1^T ....(\mathbf{e}_{j_0}^R)_{N_2}^T}_{for\ j=1,....,N_2} \mid \underbrace{(\mathbf{f}_{j_0})_1^T ....(\mathbf{f}_{j_0})_M^T}_{for\ P=1,....,M}]^T \tag{60}$$

and

$$\mathbf{U} = [\mathbf{L}_1^T ......\mathbf{L}_{N_1}^T \mid \mathbf{R}_1^T ....\mathbf{R}_{N_2}^T \mid \widehat{\mathbf{F}}_1^T ....\widehat{\mathbf{F}}_M^T]^T \tag{61}$$

The coefficients C_{j_0} may now be found as

$$C_{j_0} = \mathbf{V}_{j_0}^T \mathbf{H} \mathbf{U} \qquad \mathbf{H} = \left[\sum_{j_0=1}^{N_e} \mathbf{V}_{j_0} \mathbf{V}_{j_0}^T \right]^+ \tag{62}$$

With the coefficients C_{j_0} in hand, one may find the final homogeneous solution as

$$\hat{u}_H(x,t) = \left(\sum_{j_0=1}^{N_e} e^{\alpha_{j_0} x + \beta_{j_0} t} \mathbf{V}_{j_0}^T \right) \mathbf{HU} \tag{63}$$

In writing (59) one may use

$$\bar{\mathbf{V}}_{j_0} = \frac{1}{s_{j_0}} \mathbf{V}_{j_0} \tag{64}$$

with s_{j_0} being an appropriate scaling factor (e.g. Hermitian length see [16]). In that case

$$\hat{u}_H(x,t) = \left(\sum_{j_0=1}^{N_e} \frac{1}{s_{j_0}} e^{\alpha_{j_0} x + \beta_{j_0} t} \bar{\mathbf{V}}_{j_0}^T \right) \bar{\mathbf{H}}\mathbf{U}, \qquad \bar{\mathbf{H}} = \left[\sum_{j_0=1}^{N_e} \bar{\mathbf{V}}_{j_0} \bar{\mathbf{V}}_{j_0}^T \right]^+ \tag{65}$$

With relations (63) or (65) in hand, we must select an appropriate set of α_{j_0} and β_{j_0}. As mentioned earlier these two parameters must satisfy the characteristic equation (7) and one may be calculated in terms of another as (8) and (9). Two strategies have been suggested in [16], one based on a projection concept and another heuristically based on numerical experiences. Here we shall employ the former, and for this, we select a number of points on imaginary axis for β_{j_0} and α_{j_0}, to be used in (8) and (9) respectively, as

$$\beta_{j_0} = q_{j_0}^{\beta} \mathbf{i}, \qquad \alpha_{j_0} = q_{j_0}^{\alpha} \mathbf{i}, \qquad \mathbf{i} = \sqrt{-1} \tag{66}$$

The largeness of the scalars, i.e. $|q_{j_0}^{\beta}|$ and $|q_{j_0}^{\alpha}|$, affects the fluctuation of the EBF along t and x axes, respectively. In the case that the points on the axes are uniformly separated by Δt and Δx, one may find the bounds of $|q_{j_0}^{\beta}|$ and $|q_{j_0}^{\alpha}|$ as

$$|q_{j_0}^{\beta}| \le \frac{\pi}{2\Delta t}, \qquad |q_{j_0}^{\alpha}| \le \frac{\pi}{2\Delta x} \tag{67}$$

assuming that a single oscillation of the function, along each axis, is allowed within $4\Delta t$ and $4\Delta x$ respectively.

Having nominated a number of EBFs, we select some of them which contribute most to the solution. To this end we find direct projection of the vectors $\bar{\mathbf{V}}_{j_0}$ on $\mathbf{U}$ by defining a projection value as

$$p_{j_0} = \left| \mathbf{V}_{j_0}^T \mathbf{U} \right| \tag{68}$$

Since for a given β one may find some α_n as (8), or vice versa for a given α a number of β_m as (9) may be found, we calculate maximum projection values for each case as

$$p_{i_0}^{\beta} = \max_n \left(\left| (\mathbf{V}_{i_0}^{\alpha_n,\beta})^T \mathbf{U} \right| \right), \quad i_0 = 1, \ldots, N_{\beta} \tag{69}$$

and

$$p_{i_0}^{\alpha} = \max_m (\left|(\mathbf{V}_{i_0}^{\alpha,\beta_m})^T \mathbf{U}\right|), \quad i_0 = 1,....,N_\alpha \tag{70}$$

In above $\mathbf{V}_{i_0}^{\alpha_n,\beta}$ and $\mathbf{V}_{i_0}^{\alpha,\beta_m}$ represent two sets of arrays as defined in (60) for pairs of (α_n, β) and (α, β_m) respectively. Now we find

$$p_{\max}^{\beta} = \max_{i_0}(p_{i_0}^{\beta}), \quad p_{\max}^{\alpha} = \max_{i_0}(p_{i_0}^{\alpha}) \tag{71}$$

and choose those EBFs which have more than a certain projection value through defining ξ as

$$p_{j_0}^{\alpha} \geq \xi \times p_{\max}^{\alpha}, \quad p_{j_0}^{\beta} \geq \xi \times p_{\max}^{\beta}, \quad 0 < \xi < 1, \quad j_0 = 1,......,N_e \tag{72}$$

In this research we use $\xi = 0.25$.

4.2 Problems with source terms

As mentioned earlier, when the right hand side of (1) is non-zero we split the solution as (5) where u_P is the solution when $q \neq 0$ disregarding the boundary conditions. The idea has much in common with the dual reciprocity method (DRM) introduced for MFS method in [22, 23] using radial basis functions. However, here we shall use either EBFs or analytical functions for this purpose in a manner similar to the way we used them in [16]. In the case of using EBFs we construct u_P by first expressing the source term in terms of EBFs as

$$q(x,t) \simeq \hat{q}(x,t) = \sum_{k_0=1}^{N_q} D_{k_0} e^{\lambda_{k_0} x + \gamma_{k_0} t}, \qquad (\lambda_{k_0}, \gamma_{k_0}) \in \mathbb{C}^2 \tag{73}$$

In the above relation, the pair $(\lambda_{k_0}, \gamma_{k_0})$ represents a set of parameters which are to be chosen so that they do not satisfy the characteristic equation (7), i.e.

$$\sum_{n=0}^{N} a_n \lambda_{k_0}^n + \sum_{m=1}^{M} b_m \gamma_{k_0}^m + \sum_{n=1}^{N}\sum_{m=1}^{M} a_{nm} \lambda_{k_0}^n \gamma_{k_0}^m \neq 0 \tag{74}$$

The coefficients D_{k_0} in (73) are found by sampling the source term q on a grid of points in the domain $[x_L, x_R] \times [0,T]$. The procedure is analogous to the one introduced in [16] and thus we avoid explaining it here for the sake of brevity (see reference [16] for the way we choose the pairs $(\lambda_{k_0}, \gamma_{k_0})$). By expressing u_P in terms EBFs as

$$u_P = \sum_{k_0=1}^{N_q} G_{k_0} e^{\lambda_{k_0} x + \gamma_{k_0} t} \tag{75}$$

where G_{k_0} is found by substituting (73) and (75) in (1) as

$$G_{k_0} = \frac{D_{k_0}}{\sum_{n=0}^{N} a_n \lambda_{k_0}^n + \sum_{m=1}^{M} b_m \gamma_{k_0}^m + \sum_{n=1}^{N}\sum_{m=1}^{M} a_{nm} \lambda_{k_0}^n \gamma_{k_0}^m} \tag{76}$$

Such a particular solution has projection on the boundaries and therefore satisfaction of the boundary conditions is performed by rewriting (2), (3) and (4) as

$$\sum_{k=0}^{K_L^i} \bar{c}_{i,k} \left[\frac{\partial^k u_H}{\partial x^k}\right]_{x=x_L} = \tilde{L}_i(t), \quad \tilde{L}_i(t) = L_i(t) - \sum_{k=0}^{K_L^i} \bar{c}_{i,k} \left[\frac{\partial^k u_P}{\partial x^k}\right]_{x=x_L} \tag{77}$$

$$\sum_{k=0}^{K_R^j} \bar{d}_{j,k} \left[\frac{\partial^k u_H}{\partial x^k}\right]_{x=x_R} = \tilde{R}_j(t), \quad \tilde{R}_j(t) = R_j(t) - \sum_{k=0}^{K_R^j} \bar{d}_{j,k} \left[\frac{\partial^k u_P}{\partial x^k}\right]_{x=x_R} \tag{78}$$

$$\sum_{k=0}^{I^P} \bar{e}_{P,k} \left[\frac{\partial^k u_H}{\partial t^k}\right]_{t=0} = \tilde{F}_P(x), \quad \tilde{F}_P(x) = F_P(x) - \sum_{k=0}^{I^P} \bar{e}_{P,k} \left[\frac{\partial^k u_P}{\partial t^k}\right]_{t=0} \tag{79}$$

and substituting (75) in them. The collocation approaches may then be followed as:

Approach I

In this form, the arrays $\mathbf{L}_i$ and $\mathbf{R}_j$ in (27) are replaced with their counterparts

$$\tilde{\mathbf{L}}_i = \left[\tilde{L}_i(t_1) \quad \tilde{L}_i(t_2) \quad \ldots\ldots \quad \tilde{L}_i(t_{N_p^t})\right]^T, \quad \tilde{\mathbf{R}}_j = \left[\tilde{R}_j(t_1) \quad \tilde{R}_j(t_2) \quad \ldots\ldots \quad \tilde{R}_j(t_{N_p^t})\right]^T \tag{80}$$

we then find

$$(\tilde{h}_L)_{i,r} = \mathbf{e}_r^T \mathbf{r}\, \tilde{\mathbf{L}}_i, \quad (\tilde{h}_R)_{j,r} = \mathbf{e}_r^T \mathbf{r}\, \tilde{\mathbf{R}}_j \tag{81}$$

and replace $\mathbf{h}_r$ by $\tilde{\mathbf{h}}_r$ arranged analogously. In place of $\mathbf{C}_r$ in (35) we evaluate

$$\tilde{\mathbf{C}}_r = \mathbf{A}_{w_r}^{-1} \tilde{\mathbf{h}}_r \tag{82}$$

With the elements of $\tilde{\mathbf{C}}_r$ in hand, one may rewrite (37) by replacing $C_{r,n}$ with $\tilde{C}_{r,n}$. Now the initial boundary conditions are considered by a set of relations similar to (41) and (42) noting $F_P(x)$ should also be replaced by $\tilde{F}_P(x)$ (see (79)). In that case (43) is written as

$$\sum_l c_l B_{P,l}(x) + \tilde{\tilde{F}}_{P,l}(x) = \tilde{F}_P(x) \tag{83}$$

with $B_{P,l}(x)$ being as the one given in (44) and

$$\tilde{\tilde{F}}^P(x) = \sum_{k=0}^{I^l} \bar{e}_{P,k} \sum_{r=1}^{N_e^t} w_r^k \left(\sum_{n=1}^{N} \tilde{C}_{r,n} e^{f_n(w_r)x}\right) \tag{84}$$

The rest of formulation is similar to those given in (45) to (49) with appropriate replacement of the arrays. The final expression is as

$$\hat{u} = \left[\sum_l \left(\sum_{n=1}^{N} (\phi_l)_n e^{f_n(s_l)x + s_l t} \right) \tilde{\bar{\mathbf{B}}}_l^T \right] \bar{\mathbf{R}} (\tilde{\bar{\mathbf{F}}} - \tilde{\bar{\hat{\mathbf{F}}}}) + \sum_{r=1}^{N_e^t} \left(\sum_{n=1}^{N} C_{r,n} e^{f_n(w_r)x + w_r t} \right) + \sum_{k_0=1}^{N_q} G_{k_0} e^{\lambda_{k_0} x + \gamma_{k_0} t} \tag{85}$$

with $\tilde{\bar{\mathbf{B}}}_l^T$, $\tilde{\bar{\mathbf{F}}}$ and $\tilde{\bar{\hat{\mathbf{F}}}}$ being the counterparts of $\bar{\mathbf{B}}_l^T$, $\bar{\mathbf{F}}$ and $\bar{\hat{\mathbf{F}}}$.

Approach II

In this form, the arrays $\mathbf{L}_i$, $\mathbf{R}_j$ and $\hat{\mathbf{F}}_P$ in (53), (54) and (55) are simultaneously replaced by $\tilde{\mathbf{L}}_i$, $\tilde{\mathbf{R}}_j$ and $\tilde{\hat{\mathbf{F}}}_P$. The array $\mathbf{U}$ in (61) is replaced with

$$\tilde{\mathbf{U}} = [\tilde{\mathbf{L}}_1^T \ldots\ldots \tilde{\mathbf{L}}_{N_1}^T \mid \quad \tilde{\mathbf{R}}_1^T \ldots\ldots \tilde{\mathbf{R}}_{N_2}^T \mid \quad \tilde{\hat{\mathbf{F}}}_1^T \ldots\ldots \tilde{\hat{\mathbf{F}}}_M^T]^T \tag{86}$$

In view of (65), the final solution is then found as

$$\hat{u}(x,t) = \left(\sum_{j_0=1}^{N_e} \frac{1}{s_{j_0}} e^{\alpha_{j_0} x + \beta_{j_0} t} \bar{\mathbf{V}}_{j_0}^T \right) \bar{\mathbf{H}} \tilde{\mathbf{U}} + \sum_{k_0=1}^{N_q} G_{k_0} e^{\lambda_{k_0} x + \gamma_{k_0} t} \tag{87}$$

Next we shall introduce a marching algorithm using the two approaches explained.

5. A time marching algorithm

As explained earlier, the two introduced approaches are suitable for the solution of problems on a finite time interval $t \in [0,T]$ (see Section 4.1). The method may be used for the solution of problems with larger time intervals, $t \gg T$ through a time marching procedure. To this end, we choose a series of overlapping time intervals. The time interval may contain just a few time steps, i.e. $T = n\Delta t$. The schematic presentation of the method, using approach II, is given in Figure 2. The solution within each time interval may be obtained by one of the two approaches introduced. Let the solution be denoted by

$$\hat{u}_\xi = \hat{u}(x, t - t_\xi) \quad t \in [t_\xi, (t_\xi + T)] \quad \xi = 0,1,2,\ \ldots. \tag{88}$$

In the above relation $\hat{u}$ is the solution obtained in (85) or (87) and $\hat{u}_\xi$ is the solution within the ξth interval. Such a solution is obtained by the following boundary conditions

$$\sum_{k=0}^{K_L^i} \bar{c}_{i,k} \left[\frac{\partial^k \hat{u}_\xi}{\partial x^k} \right]_{x=x_L} = L_i(t - t_\xi), \quad i = 1,\ldots.,N_1, \quad K_L^i \in \mathbb{N}, \quad t \in [t_\xi, (t_\xi + T)] \tag{89}$$

$$\sum_{k=0}^{K_R^j} \bar{d}_{j,k} \left[\frac{\partial^k \hat{u}_\xi}{\partial x^k} \right]_{x=x_R} = R_j(t - t_\xi), \quad j = 1,\ldots.,N_2, \quad K_R^j \in \mathbb{N}, \quad t \in [t_\xi, (t_\xi + T)] \tag{90}$$

which are the same as those in (2) and (3) by considering an appropriate shift in time. Now a marching time step is chosen, e.g. $\overline{T} = \overline{n}\,\Delta t$, $\overline{n} < n$. With such a time marching step we may write

$$t_\xi = t_{\xi-1} + \overline{T} \ , \quad \overline{T} < T \tag{91}$$

The initial conditions for the current time interval are defined from the solution obtained for the previous interval i.e.

$$\left[\hat{u}_\xi\right]_{t=t_\xi} = \left[\hat{u}_{\xi-1}\right]_{t=t_{\xi-1}+\overline{T}} , \ \left[\frac{\partial \hat{u}_\xi}{\partial t}\right]_{t=t_\xi} = \left[\frac{\partial \hat{u}_{\xi-1}}{\partial t}\right]_{t=t_{\xi-1}+\overline{T}} , \ \ldots , \ \left[\frac{\partial^{M-1} \hat{u}_\xi}{\partial t^{M-1}}\right]_{t=t_\xi} = \left[\frac{\partial^{M-1} \hat{u}_{\xi-1}}{\partial t^{M-1}}\right]_{t=t_{\xi-1}+\overline{T}} \tag{92}$$

Note that the above initial conditions may be cast in a compact relation as (4). Provided that the time intervals are chosen equally, i.e. all with duration of T, the solution procedure becomes sequentially systematic with the aid of the available numerical operators/matrices obtained for the first time interval. Schematic presentation of the solution procedure is shown in Figure 2.

Remark 7: In the case that the definitions of the initial conditions in (4) differ from those in (92), the matrices obtained for the first time interval, i.e. $t \in [0, T]$, may not be used for the next interval. In such a situation, it is needed to repeat the solution procedure for $t \in [\overline{T}, (\overline{T} + T)]$. From this time on, the marching algorithm becomes sequentially systematic with the available numerical operators. ■

We shall discuss on the effects of the duration of T and $\overline{T}$ on the accuracy of the analysis while presenting the results of such time marching procedure in the sample problem 5.

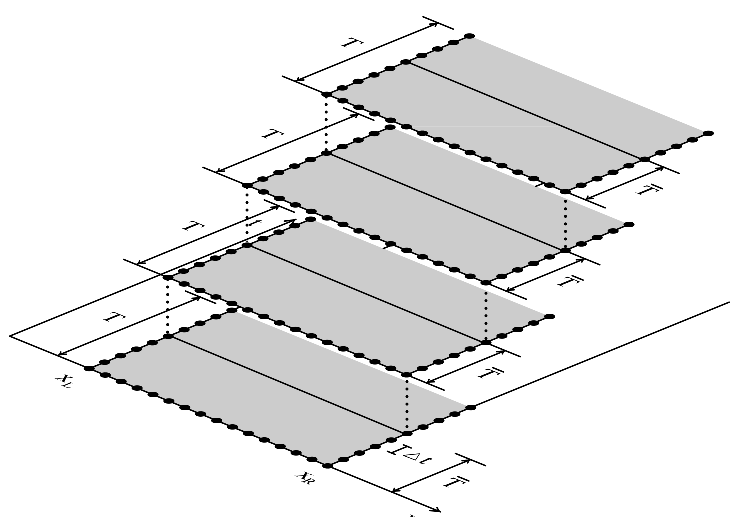

Figure 2. Schematic presentation of the proposed time marching method using approach II.

6. Application to mathematical problems

In this section we consider some mathematical problems which do not necessarily have physical interpretation.

6.1 General mathematical problems: Sample problem 1.

In Equation (1) we consider $N=3$, $M=2$ and select a_n, b_m and a_{nm} so that the following third order differential equation is defined

$$\frac{\partial^3 u}{\partial x^3}-\frac{\partial^2 u}{\partial t^2}=0 \qquad 0\le x\le L \tag{93}$$

which is to be solved with the following boundary conditions

$$\left[u\right]_{x=0}=L_1(t)\ , \qquad \left[u\right]_{x=L}=R_1(t)\,, \ \left[\frac{\partial u}{\partial x}\right]_{x=L}=R_2(t) \tag{94}$$

The above relations are arranged by considering $N_1=1$, $K_L^1=0$ and $\overline{c}_{1,0}=1$ in (2), and $N_2=2$, $K_R^1=0$, $K_R^2=1$, $\overline{d}_{1,0}=1$, $\overline{d}_{2,0}=0$ and $\overline{d}_{2,1}=1$ in (3). The initial conditions are

$$\left[u\right]_{t=0}=F_1(x)\,, \ \left[\frac{\partial u}{\partial t}\right]_{t=0}=F_2(x) \tag{95}$$

Which are arranged by choosing $M=2$, $I^{p=1}=0$, $I^{p=2}=1$, $\overline{e}_{1,0}=1$, $\overline{e}_{2,0}=0$ and $\overline{e}_{2,1}=1$ in (4).

6.1.1 Approach I

Having written the characteristic equation (7), we find α_1, α_2 and α_3 in terms of β as $f_n(\beta)$, $n=1,2,3$ in (8) as follows

$$f_1(\beta)=\beta^{2/3},\ f_2(\beta)=(-\frac{1}{2}+\frac{\sqrt{3}}{2}\mathbf{i})\beta^{2/3},\ f_3(\beta)=(-\frac{1}{2}-\frac{\sqrt{3}}{2}\mathbf{i})\beta^{2/3} \tag{96}$$

Therefore, when α is calculated in terms of β

$$\hat{u}_H\left(x,t\right)=\sum_{j_0=1}^{N_e}\left\{C_{j_0}^1 e^{\beta_i^{2/3}x+\beta_i t}+C_{j_0}^2 e^{(-\frac{1}{2}+\frac{\sqrt{3}}{2}\mathbf{i})\beta^{2/3}x+\beta_i t}+C_{j_0}^3 e^{(-\frac{1}{2}-\frac{\sqrt{3}}{2}\mathbf{i})\beta^{2/3}x+\beta_i t}\right\} \tag{97}$$

With the above relations in hand, one may find $\mathbf{A}_\beta$ through (19) to (20) and set its determinant to zero which results in the characteristic equation (21) as

$$|\,\mathbf{A}_\beta\,|=\frac{1}{2}e^{-\beta^{2/3}L}\left(-2\sqrt{3}\,\mathbf{i}+(3+\sqrt{3}\,\mathbf{i})e^{(\frac{3}{2}-\frac{\sqrt{3}}{2}\mathbf{i})\beta^{2/3}L}+(-3+\sqrt{3}\,\mathbf{i})e^{(\frac{1}{2}+\frac{\sqrt{3}}{2}\mathbf{i})\beta^{2/3}L}\right)\beta^{2/3}=0 \tag{98}$$

6.1.2 Approach II

In this approach, in addition to relation (97), we find β in terms of α as (9) and thus for this case we obtain

$$\overline{f}_1(\alpha) = +\sqrt{\alpha^3} \quad , \qquad \overline{f}_2(\alpha) = -\sqrt{\alpha^3} \tag{99}$$

We add the following forms to those in (97)

$$\hat{u}_H\left(x,t\right) = \sum_{j_0=1}^{N_e}\left\{\overline{C}_{j_0}^1 e^{\alpha_i x + \sqrt{\alpha_i^3}\,t} + \overline{C}_{j_0}^2 e^{\alpha_i x - \sqrt{\alpha_i^3}\,t}\right\} \tag{100}$$

in which $\overline{C}$ represents a new set of unknown coefficients. The procedure is continued by selecting a set of values for α and β as explained in [16]. The rest of the procedure is straightforward.

6.1.3 Numerical Solution

Now we consider an exact solution as

$$u_{exact} = x^3 + 2t\,x^2 + 3t^2 \tag{101}$$

The boundary conditions are found by inserting (101) in (94), and (95) by considering $L = 1$. For numerical solution we choose a time interval of $t \in [0,1]$. A gird of 20 nodes is used along x and a grid of 2×81 nodes ($\Delta t = 0.025$) is used along t at the two sides. In Approach I, we use the first seven set of roots of equation (98) for $\hat{u}_H^g$. For $\hat{u}_H^0$ we consider w_r as follow

$$w_r = \overline{w}\,\mathbf{i}\,, \qquad \overline{w} \in \left\{\pm 0.001, \pm 1, \ldots, \pm 9, \pm 10\right\} \tag{102}$$

Figure 3 depicts the variation of the two parts of the solution as given in (14). Figure 3-d shows the error distribution of the final solution. The maximum error is less than 0.01%.

In approach II, α_{j_0} and β_{j_0} in (60) are selected as below

$$\alpha_{j_0} = q_{j_0}^{\alpha}\mathbf{i}\,, \text{ or } \beta_{j_0} = q_{j_0}^{\beta}\mathbf{i} \qquad \left(q_{j0}^{\alpha}, q_{j0}^{\beta}\right) \in \left\{Q\right\}^2 \tag{103}$$

where $\left\{Q\right\} = \left\{\pm 0.01, \pm 1, \ldots, \pm 4, \pm 5, \pm 6\right\}$. The results obtained by Approach II are shown in Figure 4. In this problem the results obtained from Approach II are of less error than those obtained by Approach I (less than 0.001%).

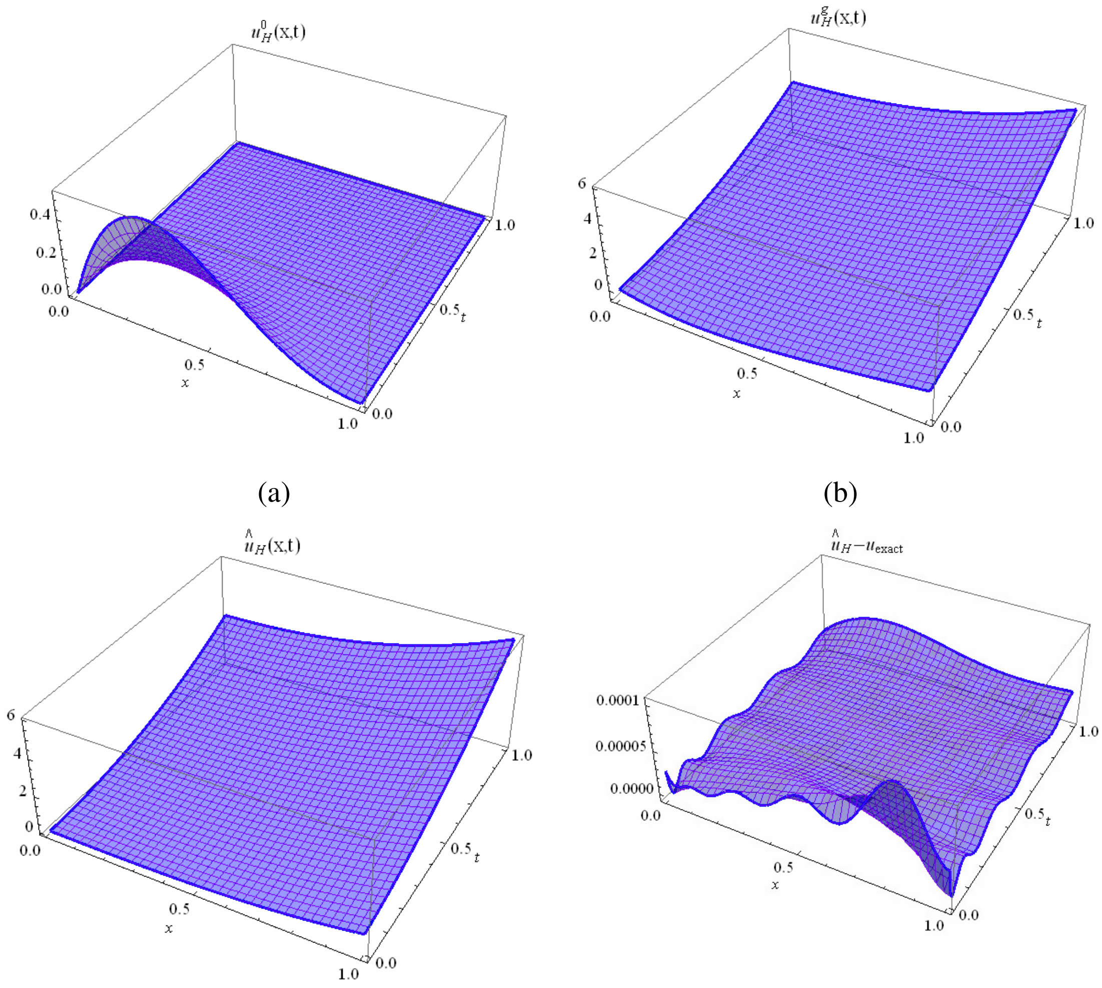

(a) (b)

(c) (d)

Figure 3. Variation of (a) $\hat{u}_H^0$, (b) $\hat{u}_H^g$, (c) $\hat{u}_H$ and (d) $u_{exact} - \hat{u}_H$ in sample problem 1 obtained from Approach I.

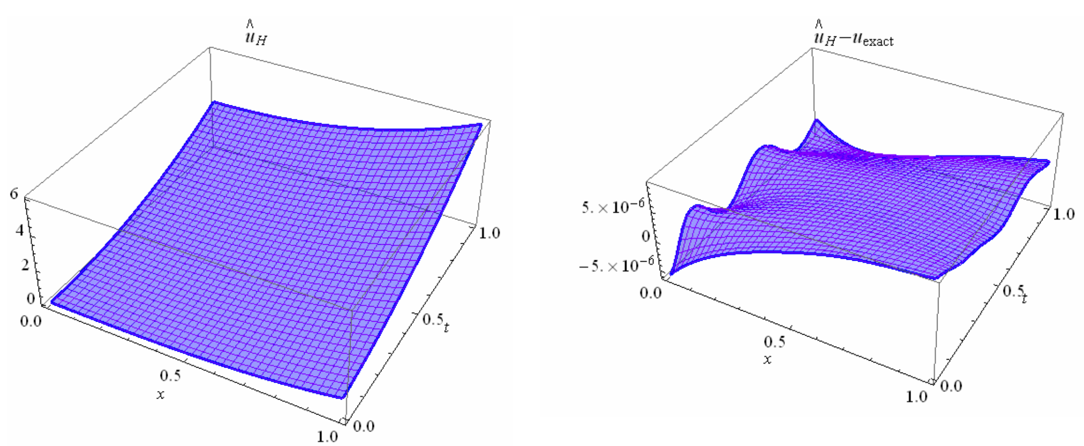

(a) (b)

Figure 4. Variation of (a) $\hat{u}_H$ and (b) $u_{exact} - \hat{u}_H$ in sample problem 1 obtained from Approach II.

6.2 General mathematical problems: Sample problem 2.

In (1) we consider $N=3$, $M=3$ and select a_n, b_m and a_{nm} so that the following third order differential equation is defined as

$$4\frac{\partial^3 u}{\partial x^3}-8\frac{\partial^3 u}{\partial x^2\partial t}+5\frac{\partial^3 u}{\partial x\partial t^2}-\frac{\partial^3 u}{\partial t^3}=0 \qquad 0\le x\le L \tag{104}$$

which is to be solved with the following boundary conditions

$$[u]_{x=0}=L_1(t)\ , \qquad [u]_{x=L}=R_1(t)\ , \quad \left[\frac{\partial u}{\partial x}\right]_{x=L}=R_2(t) \tag{105}$$

The above relations are arranged by considering $N_1=1$, $K_L^1=0$ and $\bar{c}_{1,0}=1$ in (2), and $N_2=2$, $K_R^1=0$, $K_R^2=1$, $\bar{d}_{1,0}=1$, $\bar{d}_{2,0}=0$ and $\bar{d}_{2,1}=1$ in (3). The initial conditions are

$$[u]_{t=0}=F_1(x)\,,\ \left[\frac{\partial u}{\partial t}\right]_{t=0}=F_2(x)\,,\ \left[\frac{\partial^2 u}{\partial t^2}\right]_{t=0}=F_3(x) \tag{106}$$

which are arranged by choosing $M=3$, $I^{p=1}=0$, $I^{p=2}=1$, $I^{p=1}=2$ $\bar{e}_{1,0}=1$, $\bar{e}_{2,0}=0$, $\bar{e}_{2,1}=1$, $\bar{e}_{3,0}=\bar{e}_{3,1}=0$, and $\bar{e}_{3,2}=1$ in (4). We shall employ the second approach for the solution. The characteristic equation of the problem defined in (104) is as

$$4\alpha^3-8\alpha^2\beta+5\alpha\beta^2-\beta^3=0 \tag{107}$$

When α is calculated in terms of β (or vice versa) we have

$$\alpha=\frac{\beta}{2}\ \text{(folded roots) and } \alpha=\beta \quad (\text{or } \beta=2\alpha \text{ (folded roots) and } \beta=\alpha) \tag{108}$$

The missing bases are found by considering another set of functions as

$$\hat{u}_H^i(x,t)=(a_i x+b_i t+c_i)\,e^{\alpha_i x+\beta_i t} \tag{109}$$

By inserting (109) in (104), the following relation is resulted

$$\begin{aligned}&a_i\left(4\alpha_i^3-8\alpha_i^2\beta_i+5\alpha_i\beta_i^2-\beta_i^3\right)x\,e^{\alpha_i x+\beta_i t}+b_i\left(4\alpha_i^3-8\alpha_i^2\beta_i+5\alpha_i\beta_i^2-\beta_i^3\right)t\,e^{\alpha_i x+\beta_i t}\\&+\left(a_i\left(12\alpha_i^2-16\alpha_i\beta_i+5\beta_i^2\right)-b_i\left(8\alpha_i^2-10\alpha_i\beta_i+3\beta_i^2\right)+c_i\left(4\alpha_i^3-8\alpha_i^2\beta_i+5\alpha_i\beta_i^2-\beta_i^3\right)\right)e^{\alpha_i x+\beta_i t}=0\end{aligned} \tag{110}$$

Inserting $\alpha=\beta/2$ (or $\beta=2\alpha$) in (110), it is found that a_i, b_i and c_i can be chosen arbitrarily (note that at least one of the first two parameters should be non zero). Here we consider $a_i=b_i=c_i$. Therefore, considering the two forms we have

$$\hat{u}_H(x,t)=\sum_{j_0=1}^{N_e}\left\{C_{j_0}^1 e^{\beta_i\left(\frac{x}{2}+t\right)}+C_{j_0}^2(x+t+1)e^{\beta_i\left(\frac{x}{2}+t\right)}+C_{j_0}^3 e^{\beta_i(x+t)}\right\}+$$
$$\sum_{j_0=1}^{N_e}\left\{\bar{C}_{j_0}^1 e^{\alpha_i(x+2t)}+\bar{C}_{j_0}^2(x+t+1)e^{\alpha_i(x+2t)}+\bar{C}_{j_0}^3 e^{\alpha_i(x+t)}\right\} \quad (111)$$

with C and $\bar{C}$ representing two sets of unknown coefficients The rest of the procedure is straightforward.

6.2.1 Numerical solution

Now we consider the following exact solution

$$u_{exact}=2xt-4t^2x+x^3-tx^2+\sin[3\pi x]\cos[3\pi t]+\sin[3\pi t]\cos[3\pi x] \quad (112)$$

The boundary conditions are found by inserting (112) in (104), (105), (106) while considering $L=1$. For numerical solution we choose $T=1.5$ and a time interval of $t\in[0,T_1=1]$ to study the results. A gird of 80 nodes is used along x and along t we use $\Delta t=0.01$. In approach II, α_{j_0} and β_{j_0} in (60) are selected as (103), respectively, while $\{Q\}=\{\pm 0.01,\pm 0.5,\ldots,\pm 9.5,\pm 10\}$. The results obtained by Approach II are shown in Figure 5. As is seen, the errors are less than 0.005% in all points.

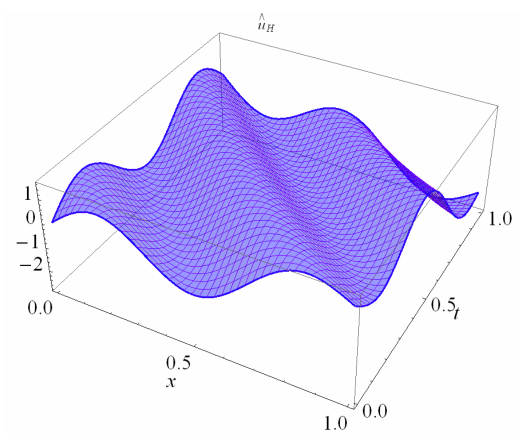

(a)

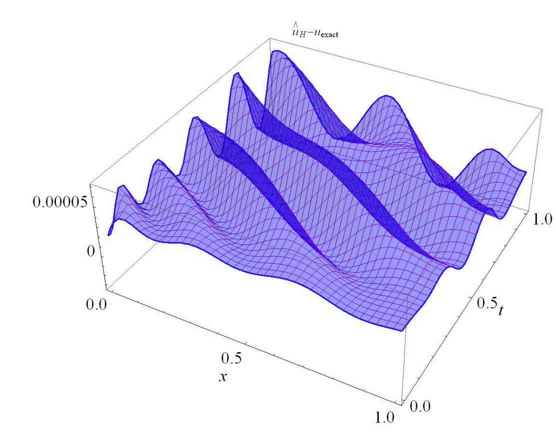

(b)

Figure 5. Variation of (a) $\hat{u}_H$ and (b) $u_{exact}-\hat{u}_H$ in sample problem 2 obtained from Approach II.

7. Application to engineering problems

In this section we consider problems which have physical interpretation.

7.1 Heat conduction problems: Sample problem 3.

In (1) consider $N=2$ and $M=1$ (with non zero coefficients as $a_2=-1$ $b_1=1$) on a domain $x_L=0$, $x_R=L$ which results in a second order differential equation known as heat conduction problem as

$$\frac{\partial u}{\partial t}-\frac{\partial^2 u}{\partial x^2}=q(x,t) \qquad 0\le x\le L \tag{113}$$

The boundary conditions are here defined as

$$[u]_{x=0}=L_1(t)\ ,\quad [u]_{x=L}=R_1(t) \tag{114}$$

which are arranged by considering $N_1=1$, $K_L^1=0$ and $\bar{c}_{1,0}=1$ in (2), and $N_2=1$, $K_R^1=0$ and $\bar{d}_{1,0}=1$ in (3). The initial condition is

$$[u]_{t=0}=F_1(x)\,, \tag{115}$$

which is arranged by choosing $I_P^1=0$ and $\bar{e}_{1,0}=1$ in (4).

7.1.1 Approach I

The parameters α_1 and α_2 are found in terms of β as

$$f_1(\beta)=+\sqrt{\beta}\ ,\quad f_2(\beta)=-\sqrt{\beta} \tag{116}$$

Evaluation of $\mathbf{A}_\beta$ through (19) to (20) and setting its determinant to zero results in the following characteristic equation

$$\sinh\left(L\sqrt{\beta}\right)=0 \tag{117}$$

from which a series of eigenvalues and eigenvectors are found as

$$\beta_l=-\left(\frac{l\pi}{L}\right)^2\ ,\quad \boldsymbol{\phi}_l^T=\{1,-1\},\quad l\in\mathbb{N} \tag{118}$$

The formulation is obviously equivalent to the use of Fourier sine series since the problems with the homogeneous boundary conditions is in fact a proper Sturm-Liouville one (see [9, 10] and also Remark 2). Nevertheless, as will be seen later, we satisfy the boundary and initial conditions according to the proposed method.

7.1.2 Approach II

In this approach, in addition to (116), we find β in terms of α (see (9)) as

$$\bar{f}_1(\alpha) = \alpha^2 \tag{119}$$

The EBFs constructed by the above relations are added to those obtained in (116). The main part of the rest of the procedure is to choose a set of points along x and t.

7.1.3 Numerical solution

We consider the following exact solution (see also [24])

$$u_{exact} = 2e^{-4t}\left(\sin(2x)+\cos(2x)\right)+3\left(t^2+t\,x+\frac{1}{12}x^4\right) \quad x\in[0,1] \quad t\in[0,1] \tag{120}$$

In this example we use 20 boundary nodes along x and different values for Δt to discretize the boundaries at $x=0$ and $x=1$. In Approach I we use $w_r \in \{\pm 0.001, \pm 1, \ldots, \pm 7, \pm 8\}\times \mathbf{i}$ and $s_l = -l^2\pi^2/L^2$, $l = 1,2,\cdots,6$ which results in a set of 12 EBFs for $\hat{u}_H^0$ and 32 EBFs for $\hat{u}_H^g$. The results obtained by Approach I with $\Delta t = 0.01$ are shown in Figure 6. The distributions of $\hat{u}_H^0$, $\hat{u}_H^g$ and $\hat{u}_H$ are shown in Figure 6-a, 6-b and 6-c. As is seen Figure 6-d, the errors are less than $0.005\,\%$ in all points.

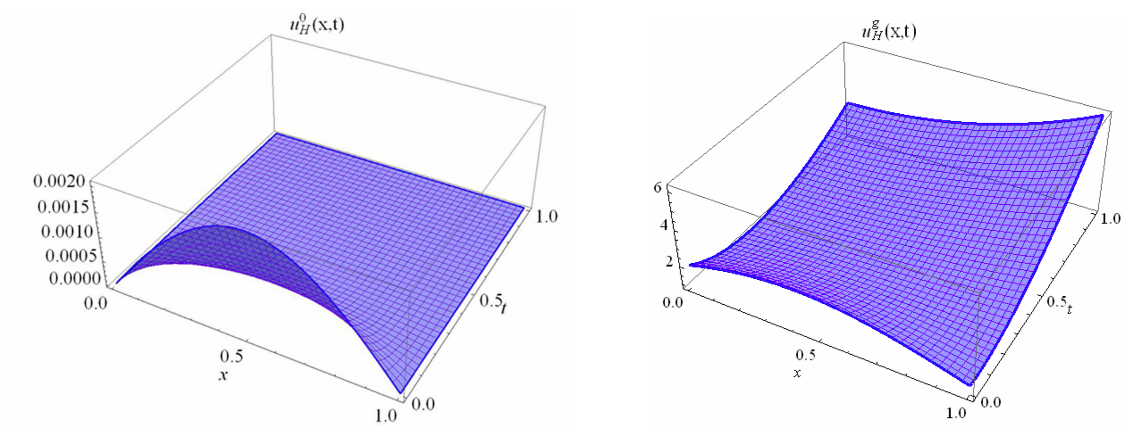

(a) (b)

Figure 6. Continued.

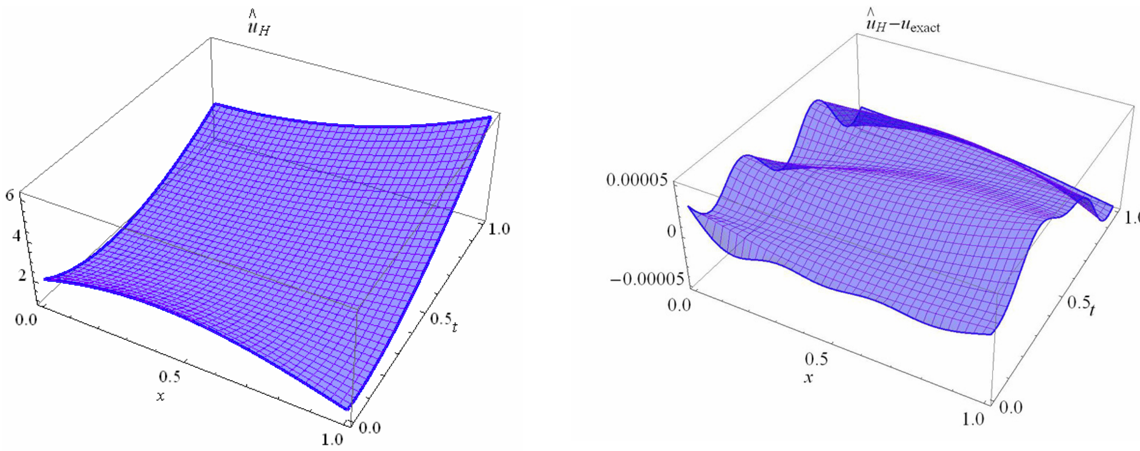

(c) (d)

Figure 6. Variation of (a) $\hat{u}_H^0$, (b) $\hat{u}_H^g$, (c) $\hat{u}_H$ and (d) $\hat{u}_H - u_{exact}$ in sample problem 3 obtained from Approach I ($\Delta t = 0.01$).

The solution is repeated using approach II. In this approach the selection of the EBFs is performed initially by the calculation of the minimum period of variations of the exponential functions and then $p_{i_0}^{\alpha}$ and $p_{i_0}^{\beta}$ as in (65) and (66). The variations of these projections are shown in Figure 7.

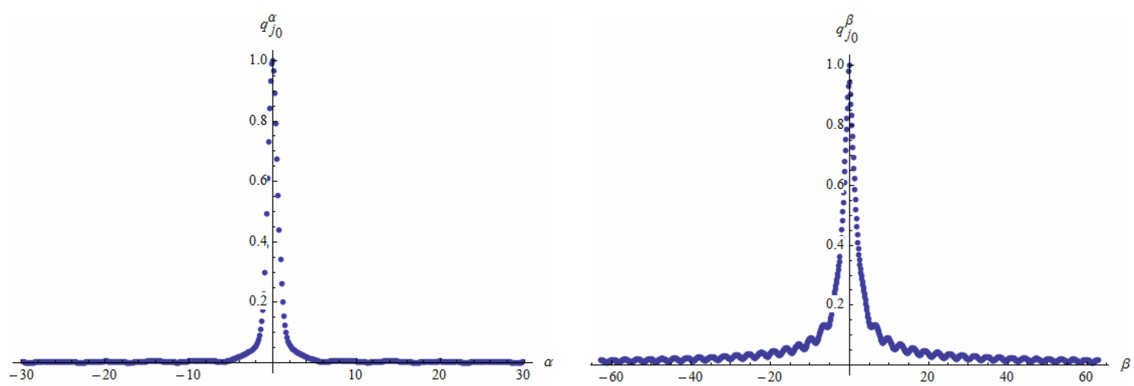

(a) (b)

Figure 7. Variation of (a) $q_{j_0}^{\alpha}$ and (b) $q_{j_0}^{\beta}$ in (66).

By considering $\xi = 0.25$, appropriate intervals for $q_{j_0}^{\alpha}$ and $q_{j_0}^{\beta}$ in (66) can be specified as $q_{j0}^{\alpha} \in \{\pm 1, \pm 2, \pm 3\}$ and $q_{j0}^{\beta} \in \{\pm 1, ..., \pm 4, \pm 5\}$ which leads to a set of 32 EBFs . The error distribution of this approach with $\Delta t = 0.01$ is illustrated in Figure 8. As is seen the errors are less than $0.0005\,\%$ in all points. Comparing with the results of Figure 6-c, it can be seen that in this example the errors in second approach are of one logarithmic order less than that of the first approach.

In Table 1 the error norms of two approaches of EBFs method are shown for five different time steps. The following norms are defined

$$\eta = \left\{ \left[\sum (u^{exact} - \hat{u})^2 \right] \Big/ \sum (u^{exact})^2 \right\}^{1/2} \ , \ e^{ave} = \left\{ \left[\sum (u^{exact} - \hat{u})^2 \right] \Big/ DP \right\}^{1/2} \quad (121)$$

In the above relations, DP denotes the number of domain points used for the norm. The norms in Table 1 are calculated on 416 domain points inside the domain. The table shows that while all the errors are reasonably low the errors in Approach II are less than those in Approach II by one logarithmic order.

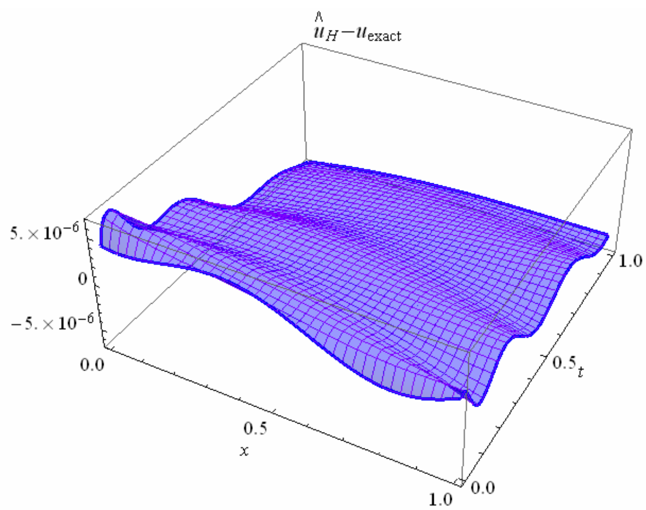

Figure 8. Variation of $u_{exact} - \hat{u}_H$ in sample problem 3 obtained from Approach II ($\Delta t = 0.01$).

Table 1. The error norms in sample problem 3 for different time steps.

Time step	Approach I		Approach II	
	e^{ave}	η	e^{ave}	η
$\Delta t = 0.2$	1.92×10^{-3}	3.35×10^{-4}	1.17×10^{-4}	4.19×10^{-5}
$\Delta t = 0.1$	9.49×10^{-5}	3.81×10^{-5}	1.20×10^{-5}	4.17×10^{-6}
$\Delta t = 0.05$	4.88×10^{-5}	1.73×10^{-5}	7.59×10^{-6}	2.92×10^{-6}
$\Delta t = 0.025$	2.25×10^{-5}	6.59×10^{-6}	5.05×10^{-6}	1.62×10^{-6}
$\Delta t = 0.01$	2.35×10^{-5}	9.18×10^{-6}	3.24×10^{-6}	8.81×10^{-7}

Also from the results of Table 1 it can be seen that the magnitude of error norms decreases when time steps with smaller size are used. However, in smaller time steps the rate of reduction in error decreases and in some cases the error remains almost constant.

7.2 Heat conduction problems: Sample problem 4.

In this example we consider the heat conduction equation in its non-homogeneous form. To this end two exact solutions and associated source functions are considered as given in Table 2 (see also [14]). Boundary conditions may be calculated from these exact solutions by considering $L=1$ and $T=1$. Twelve boundary nodes are selected along x and the time step Δt, is chosen as 0.025. In order to evaluate the heat source functions, $q(x,t)$, 128 uniformly distributed domain points are selected inside the domain. Here again the solution is performed using the two approaches. Initially the heat source functions, $q(x,t)$, is expressed in terms of exponential basis functions. The bases are produced by considering the parameters listed in Table 2.

Table 2. Exact solutions with heat source in sample problem 4.

No. of exact solution	$u(x,t)$	$q(x,t)$
1	$\left(x-e^{-t}\right)\sin(x)$	$x\sin(x)-2\cos(x)$
2	$e^{-3t}x^4$	$-3e^{-3t}x^2\left(4+x^2\right)$

The errors of the approximated source term, $\hat{q}(x,t)$, as given in (73) are given in Table 3 (the definition of η_q is similar to η in (121) with u replaced by q). The norms are calculated on 676 points.

Table 3. The errors of the approximated source terms in sample problem 4.

No. of exact solution	Number of EBFs	e^{ave}	η_q
1	90	5.98884×10^{-6}	4.04787×10^{-6}
2	168	5.28902×10^{-5}	1.9014×10^{-5}

In Table 4, we summarize the parameters used and the errors obtained from the two approaches. In this example the errors of Approach I are less than those of Approach II.

Table 4. The parameters used for homogenous solution of sample problem 4.

	Exact solution		Parameters used	The No. of bases	e^{ave}	η
Approach I	1	$\hat{u}_H^0$	$s_l = -l^2\pi^2/L^2 \quad l = 1,2,\cdots,5$	10	4.32×10^{-7}	2.75×10^{-6}
		$\hat{u}_H^g$	$w_r \in \{\pm0.001,\pm0.5,\cdots,\pm2.5,\pm3\}\times\mathbf{i}$	24		
	2	$\hat{u}_H^0$	$s_l = -l^2\pi^2/L^2 \quad l = 1,2,\cdots,7$	14	1.89×10^{-4}	1.25×10^{-3}
		$\hat{u}_H^g$	$w_r \in \{\pm0.001,\pm0.5,\cdots,\pm8.5,\pm9\}\times\mathbf{i}$	72		
Approach II	1		$\left(q_{j_0}^{\alpha}\right)q_{j_0}^{\beta} \in \{0,\pm2,\pm4,\pm6,\pm8\}$	30	2.71×10^{-6}	1.72×10^{-5}
	2		$\left(q_{j_0}^{\alpha}\right)q_{j_0}^{\beta} \in \{0,\pm1,\pm2,\cdots,\pm6\}$	42	7.32×10^{-4}	4.84×10^{-3}

7.3 Wave propagation problems: Sample problem 5.

Again in Equation (1) we consider, $N = 2$, $M = 2$ and select a_n, b_m and a_{nm} so that the following second order differential equation, known as wave equation, is defined

$$\frac{\partial^2 u}{\partial t^2} - \frac{\partial^2 u}{\partial x^2} = q(x,t) \qquad 0 \le x \le L \tag{122}$$

The boundary conditions are defined as

$$[u]_{x=0} = L_1(t) \qquad [u]_{x=L} = R_1(t) \tag{123}$$

which are arranged by considering $N_1 = 1$, $K_L^1 = 0$ and $\bar{c}_{1,0} = 1$ in (2), and $N_2 = 1$, $K_R^1 = 0$ and $\bar{d}_{1,0} = 1$ in (3). The initial condition is

$$[u]_{t=0} = F_1(x), \qquad \left[\frac{\partial u}{\partial t}\right]_{t=0} = F_2(x) \tag{124}$$

which is arranged by choosing $I_P^1 = 0$ and $\bar{e}_{1,0} = 1$ and $I_P^2 = 1$ and $\bar{e}_{2,0} = 0$, $\bar{e}_{2,1} = 1$ in (4).

7.3.1 Approach I

The parameters α_1 and α_2 are found in terms of β as

$$f_1(\beta) = +\beta, \; f_2(\beta) = -\beta \tag{125}$$

Evaluation of $\mathbf{A}_\beta$ through (19) to (20) and setting its determinant to zero results in the following characteristic equation

$$\sinh(L\beta) = 0 \tag{126}$$

from which a series of eigenvalues and eigenvectors are found as

$$\beta_l = \frac{l\,\mathbf{i}\,\pi}{L} \quad , \quad \boldsymbol{\phi}_l^T = \{1,-1\}, \quad l \in \mathbb{Z} \tag{127}$$

7.3.2 The use of Fourier series

In standard wave problems as defined in (122), (123) and (124), approach I of our method has much in common with Sturm-Liouville problems. In view of (127), we find $\hat{u}_H^0$ as the following expression

$$\hat{u}_H^0 = \sum_{s=1}^{\infty} \left\{ c_1^s e^{\frac{s\mathrm{i}\pi}{L}t} + c_2^s e^{-\frac{s\mathrm{i}\pi}{L}t} \right\} \sin\left(\frac{s\pi x}{L}\right) \tag{128}$$

Likewise for $\hat{u}_H^g$ we write

$$\hat{u}_H^g = \sum_{r=-\infty}^{\infty} \left\{ d_1^r e^{\frac{2r\mathrm{i}\pi}{T}x} + d_2^r e^{-\frac{2r\mathrm{i}\pi}{T}x} \right\} e^{\frac{2r\mathrm{i}\pi}{T}t}, \qquad \frac{2r}{T} \neq \frac{s}{L} \tag{129}$$

In (128) and (129), c_1^s, c_2^s, d_1^r and d_2^r are found from boundary conditions which are expressed in terms of Fourier series (see (38) and (39)). For instance

$$F_P(x) = \sum_{s=0}^{\infty} F_{P_s} \sin\left(\frac{s\pi}{L}x\right), \quad F_{P_s} = \frac{2}{L}\int_L F_P(x)\sin\left(\frac{s\pi}{L}x\right)dx, \quad P = 1,2$$

In this form of solution no collocation scheme is used neither along x nor along t. The rest of the procedure is straightforward. We shall compare the results with those of Approach I.

7.3.3 Approach I incorporating Fourier series in time (a hybrid method)

In this hybrid form we use Fourier series in time as given in (38) and (39) to find $\hat{u}_H^g$ and use a collocation scheme along x axis as explained in Approach I. The aim is to compare the results of the results with those obtained with Approach I.

7.3.4 Approach II

Formulation of approach II for wave equation is similar to that already mentioned. Again, we find β in terms of α (see (9)) as

$$\overline{f}_1(\alpha) = \alpha, \qquad \overline{f}_2(\alpha) = -\alpha \tag{130}$$

The EBFs constructed by the above relations are added to those obtained in (125).

7.3.5 Numerical solution

We consider the following exact solution

$$u_{exact} = -3x^3 + 5x^4 - 9xt^2 + 30x^2t^2 + 5t^4 + 20\sin(7x)\sin(7t), \quad x \in [0,1], \qquad t \in [0,1] \tag{131}$$

For approaches I and II we use 20 boundary nodes on initial boundary and $\Delta \mathrm{t} = 0.005$. Prior to solution of the problem we examine the performance of Fourier series and the collocation method in reproducing the non-homogenous side boundary conditions $L_1(t)$ and $R_1(t)$. Figure 9 depicts the variation of L_2 norm of the errors in terms of the number of bases used in Fourier series or those in Approach I. As is seen, the collocation scheme used in Approach I can reproduce the functions with high accuracy and less number of EBFs. In Table 5 we summarize the error norms calculated for the solution with Fourier series for the problem. Table 6 shows the results obtained from the two approaches proposed. By comparing the contents of Tables 5 and 6 it can be realized that the presented method is capable of giving more accurate results with less number of bases. The results of the hybrid approach, i.e. use of Fourier series combined with Approach I, are presented in Table 7. As is seen, the errors are of twice as much as those in Table 6 but are much less than those in Table 5. To give more insight to the solution methods, we present the variation of the exact solution and the errors in Figure 10.

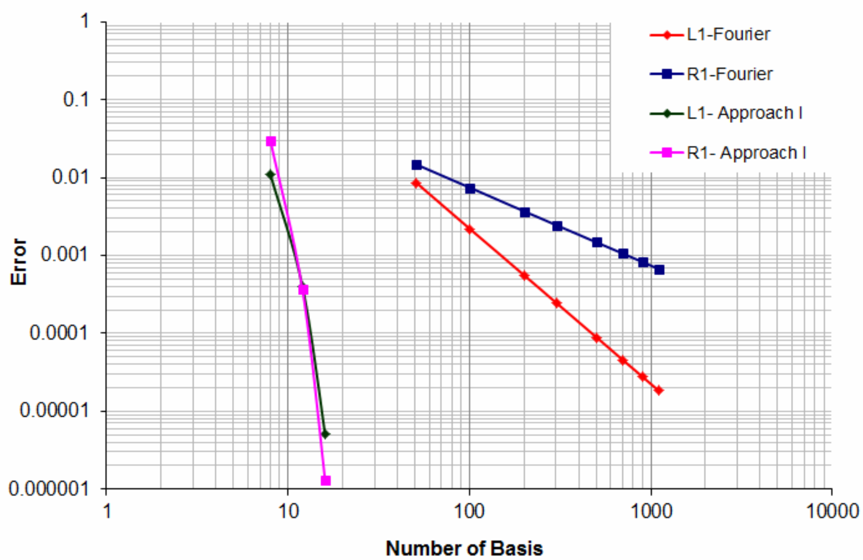

Figure 9. Variation of L_2 norm of errors in approximated side boundary values, $L_1(t)$ and $R_1(t)$, in terms of the number of bases used in Fourier series and those in Approach I.

Table 5. The error norms of the solution using Fourier series in sample problem 5 (Error norms are calculated on 196 domain points).

N_r	N_s	e^{ave}	η
101	50	1.69E-2	4.71E-4
201	100	7.19E-3	2.01E-4
701	350	2.16E-3	6.05E-5

N_r denotes the Number of bases in complex Fourier series used for $\hat{u}_H^g$ (see (38) and (39))

N_s denotes the Number of bases in sine Fourier series used for $\hat{u}_H^0$

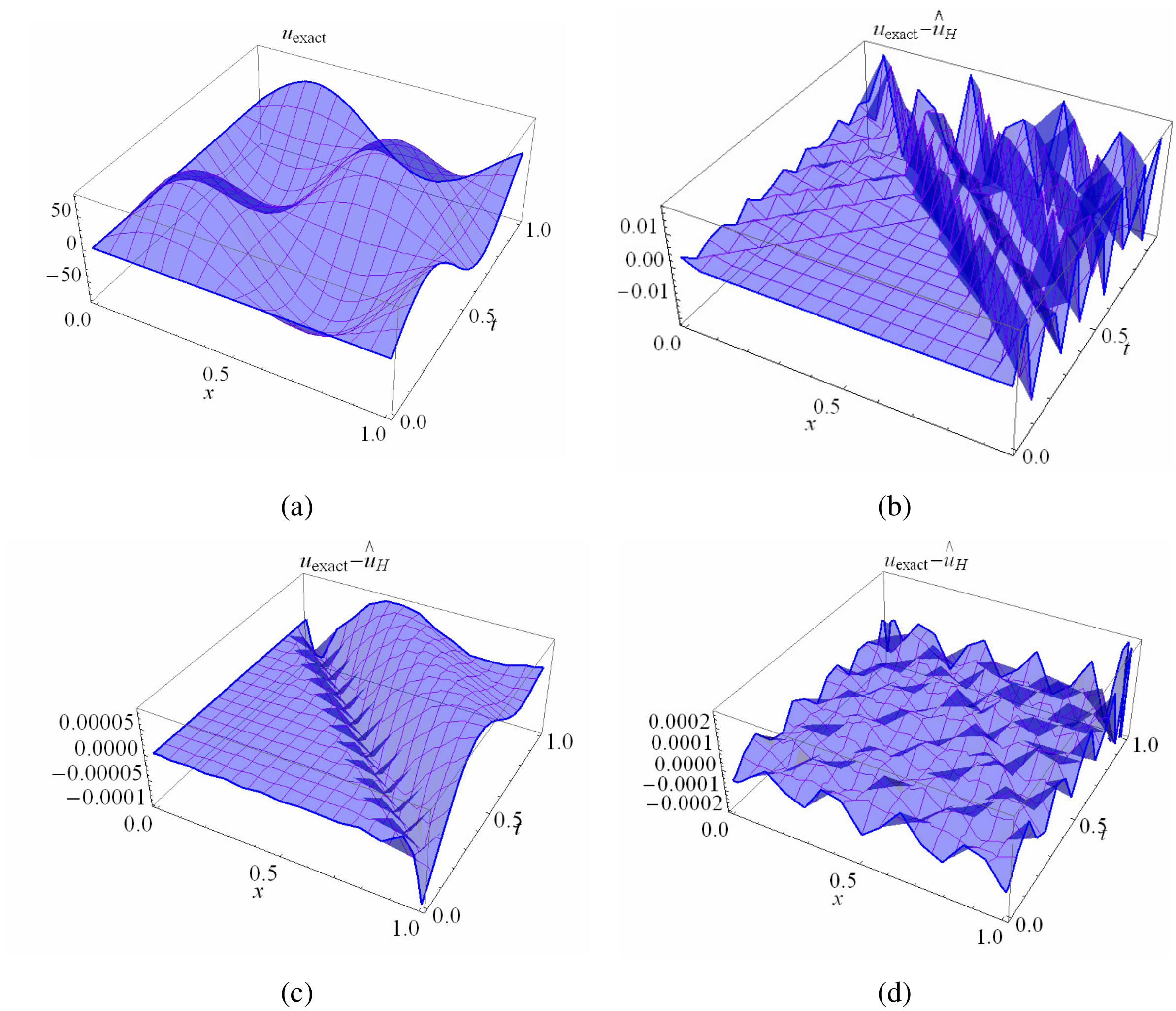

Figure 10. Variation of (a) exact solution, (b) error of Fourier series method (2nd row of Table 5) (c) error of Approach I and (d) error of Approach II (sample problem 5).

Table 6. The parameters used and the results of the two approaches in solution of sample problem 5 (Error norms are calculated on 196 domain points).

Approach		Parameters used	No. of EBFs	e^{ave}	η
No. I	$\hat{u}_H^0$	$s_l = -l\,\mathbf{i}\,\pi / L, \qquad l = 1,2,\cdots,15$	30	4.02E-5	1.13E-6
	$\hat{u}_H^g$	$w_r \in \{\pm 0.005, \pm 1, \cdots, \pm 7, \pm 8\} \times \mathbf{i}$	16		
No. II		$\alpha_{j_0} = q_{j_0}^{\alpha}\mathbf{i}, \quad \beta_{j_0} = q_{j_0}^{\beta}\mathbf{i}$ $\left(q_{j_0}^{\alpha}\right) q_{j_0}^{\beta} \in \{\pm 2, \ldots, \pm 18, \pm 20, \pm 22\}$	88	5.16E-5	1.45E-6

Table 7. The parameters used and the results of the hybrid approach in solution of sample problem 5 (Error norms are calculated on 196 domain points).

No. of EBFs for $\hat{u}_H^g$	N_s	e^{ave}	η
32 $w_r \in \{\pm 0.005, \pm 1, \cdots, \pm 7.5, \pm 8\} \times \mathbf{i}$	50	1.21E-4	3.39E-6
	150	1.21E-4	3.40E-6
	250	1.21E-4	3.40E-6

N_r denotes the Number of bases in complex Fourier series used for $\hat{u}_H^g$ (see (38) and (39))

Now we reconsider the problem with longer time period, $t \in [0,8]$, and apply the time marching algorithm proposed in [1]. We shall use approach I to solve the problem within smaller time intervals T. A marching step $\overline{T}$ is also chosen (see Fig 2). For construction of $\hat{u}_H^g$ we use $w_r \in \{\pm 0.005, \pm 0.25, \cdots, \pm 8.75, \pm 9\} \times \mathbf{i}$ and 40 nodes for initial boundary conditions. Figure 11 depicts the variation of error norm, as defined in (121), in terms of the number of marching steps (here defined as $n_s = t_{\max} / \overline{T}$) and various time intervals. The errors are calculated on 1640 points. It can be seen that for small number of time steps the errors of the three time intervals are rather similar. Note that for $T = t_{\max} = 8$, just one time interval is used meaning that the solution is performed with no marching procedure. For larger number of time steps, the errors obtained for two time intervals, i.e. $T = 2 = t_{\max}/4$ and $T = 1 = t_{\max}/8$ significantly differ from the those of $T = t_{\max}$ (about three logarithmic order smaller). It is worthwhile to mention that the times consumed for $T = 2$ and $T = 1$ for $n_s = 640$ are less than about a half and two third, respectively, of the time consumed for $T = t_{\max}$ in this problem.

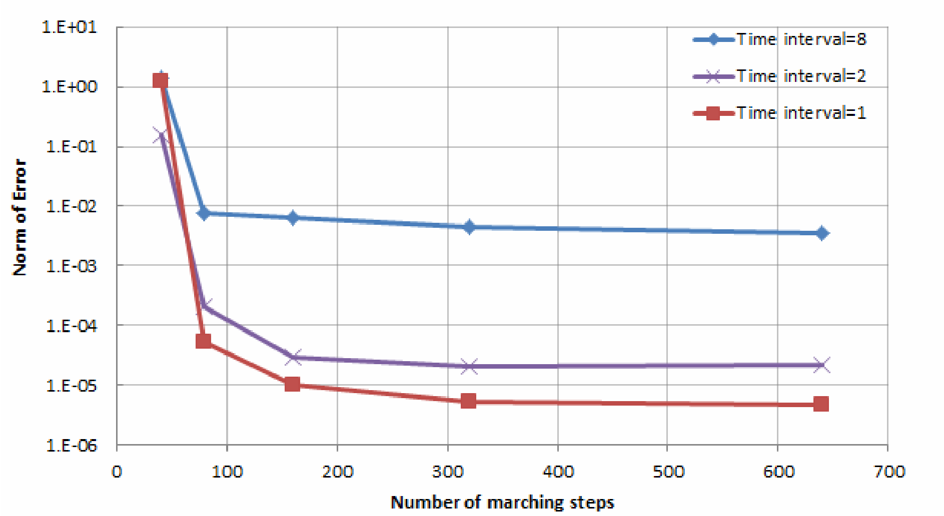

Figure 11. The variation of error norm in solution of Sample problem 5 with $t \in [0,8]$ **using the proposed time marching algorithm.**

7.4 Wave propagation problems: Sample problem 6.

In this problem we study the vibration of a straight bar with two lumped masses and two springs at both ends as shown in Figure 12. The governing equation of this problem and its boundary conditions can be considered as follows

$$E\frac{d^2u}{dx^2}-\rho\frac{d^2u}{dt^2}=0 \qquad x_L=0,\ x_R=L \tag{132}$$

$$\left[-\frac{M_1E}{\rho}\frac{d^2u}{dx^2}+EA\frac{du}{dx}-K_1u\right]_{x=0}=L_1(t),\quad \left[-\frac{M_2E}{\rho}\frac{d^2u}{dx^2}-EA\frac{du}{dx}-K_2u\right]_{x=L}=R_1(t) \tag{133}$$

The initial conditions are

$$[u]_{t=0}=F_1(x),\ \left[\frac{\partial u}{\partial t}\right]_{t=0}=F_2(x) \tag{134}$$

3.4.1 Approach I

The parameters α_1 and α_2 are found in terms of β as

$$f_1(\beta)=+\sqrt{\frac{\rho}{E}}\beta,\ f_2(\beta)=-\sqrt{\frac{\rho}{E}}\beta \tag{135}$$

By evaluating $\mathbf{A}_\beta$ through (19) to (20) and setting its determinant to zero, the following characteristic equation is resulted

$$\begin{aligned}&\frac{E\beta e^{-L\beta}}{\rho^2}\{E\beta\big((M_1\beta-\rho A)(M_2\beta-\rho A)-e^{2L\beta}(M_1\beta+\rho A)(M_2\beta+\rho A)\big)\\&+\rho\big(-2K_2\rho A+K_1\big(M_2\beta-\rho A-e^{2L\beta}(M_2\beta+\rho A)\big)\big)\}=0\end{aligned} \tag{136}$$

If we assume $\beta = s\,\mathbf{i}$, then (136) converts to the following equation

$$\begin{aligned}&\frac{E\,s\,e^{-isL}}{\rho^2}\{-\mathbf{i}\,K_1\rho^2 A\left(1+e^{2\mathrm{i}sL}\right)+2\,\mathbf{i}\,e^{\mathrm{i}sL}\{\rho A\left(E\left(M_1+M_2\right)s^2-K_2\rho\right)cos\left(L\,s\right)\\&+\left(-E\,M_1 M_2 s^3+K_1 M_2\,\rho\,s+\rho^2 A\left(\mathbf{i}\,K_2+EA\,s\,\right)\right)\sin\left(L\,s\right)\}\}=0\end{aligned} \tag{137}$$

We use a numerical method to solve the following equation and find a series of eigenvalues and eigenvectors of $\mathbf{A}_\beta$.

7.4.2 Approach II

Here again, we find β in terms of α as

$$\bar{f}_1(\alpha)=\sqrt{\frac{E}{\rho}}\alpha, \qquad \bar{f}_2(\alpha)=-\sqrt{\frac{E}{\rho}}\alpha \tag{138}$$

and add them to those obtained in (135).

7.4.3 Numerical solution

For a numerical solution we consider $M_1 = M_2 = K_1 = K_2 = \rho = E = A = 1$, $L_1(t) = R_1(t) = 0$ and $F_1(x) = 0.1 + 0.1\,x/L$, $F_2(x) = 0$.

It should be noted that there is no exact solution for this example. Here the aim is to provide a benchmark problem for further studies. We shall solve the problem using Approach I of presented method. 60 boundary nodes are selected along x. The displacements obtained for the two masses are shown in Figure 13. Similar results are obtained with the time marching algorithm using approach II ($T = 1$, $\bar{T} = 0.5$).

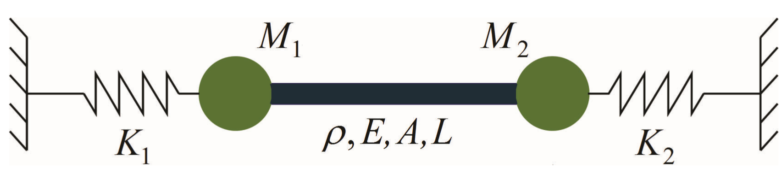

Figure 12. The model of sample problem 6.

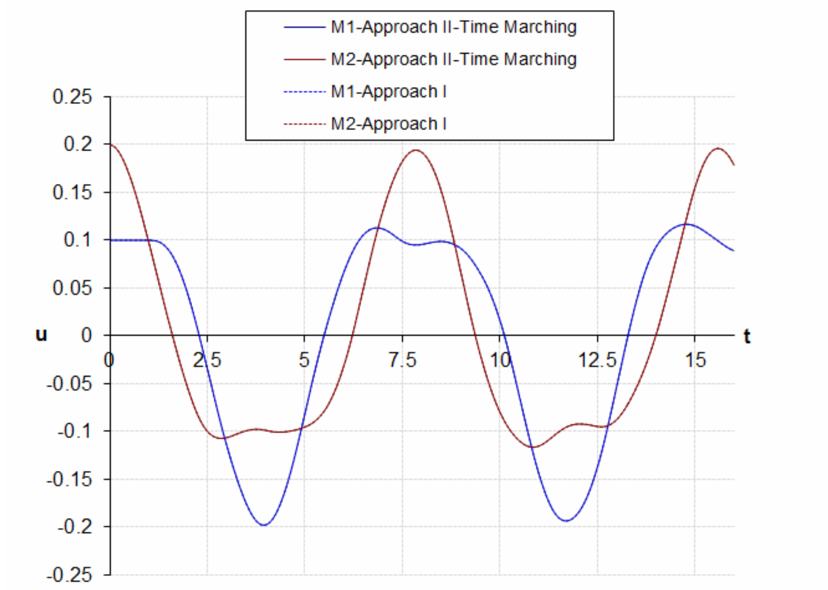

Figure 13. Displacement of M_1 and M_2 in sample problem 6 obtained from Approach I (and time marching algorithm using Approach II).

7.5 Wave propagation problems: Sample problem 7.

In this last example we demonstrate the capability of the method in the solution of problems with moving boundaries. Here again we introduce a benchmark wave problem with governing equation as (122) with the exact solution as follows

$$u_{exact} = e^{-t} \sin\left(\pi\left(x+t\right)\right) \sin\left(\pi\left(x-t\right)\right) \tag{139}$$

The boundary conditions are as (123) with $L_1(t) = R_1(t) = 0$, however, the position of the two ends varies with time as

$$x_L\left(t\right) = -t \ , \ x_R\left(t\right) = t+1 \tag{140}$$

The right side functions in (123) is as

$$q\left(x,t\right) = -e^{-t}\left(2\pi\cos\left(\pi\left(x-t\right)\right) + \sin\left(\pi\left(x-t\right)\right)\right) \times \left(2\pi\cos\left(\pi\left(x+t\right)\right) - \sin\left(\pi\left(x+t\right)\right)\right) \tag{141}$$

Figure 14-a shows the arrangement of boundary nodes on initial and side boundaries. In this example 20 boundary nodes are used at initial boundary and the time step is selected as $\Delta t = 0.025$.

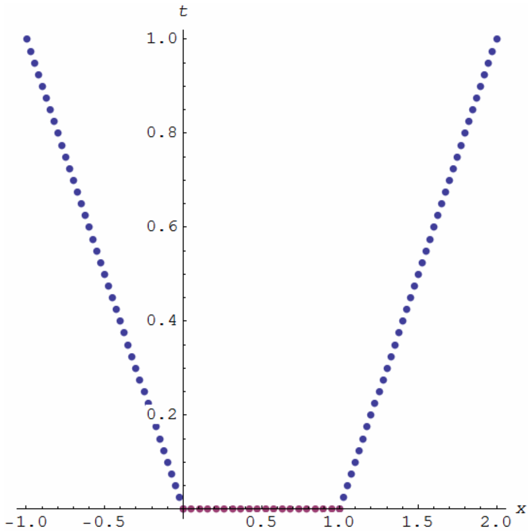

(a)

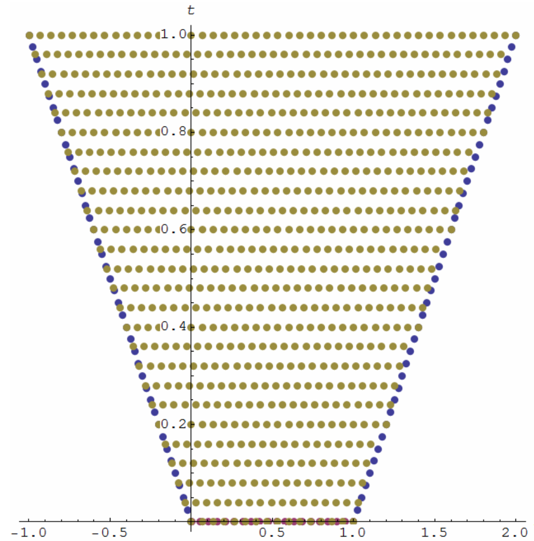

(b)

Figure 14. Distribution of (a) boundary nodes, (b) domain points for calculation of two error norms in sample problem 7.

The parameters used for construction of EBFs are shown in Table 8. The error norms are calculated on 796 points inside the domain (Figure 14-b). We solve the problem with approach II since the boundary points are moving and Approach I is not applicable. Figure 15 depicts the variation of the solution obtained and the errors distribution. The error norms are given in Table 8. As seen the proposed method is capable of finding the solution with high accuracy.

Table 8. The parameters used to solve sample problem 7 by Approach II.

	Parameters	No. of EBFs	e^{ave}	η
Homogenous solution	$\alpha_{j_0} = q^{\alpha}_{j_0}\mathbf{i}$, $\beta_{j_0} = q^{\beta}_{j_0}\mathbf{i}$ $\left(q^{\alpha}_{j_0}\right) q^{\beta}_{j_0} \in \{0, \pm 1, \ldots, \pm 7, \pm 8\}$	72	9.4×10^{-6}	3.1×10^{-5}

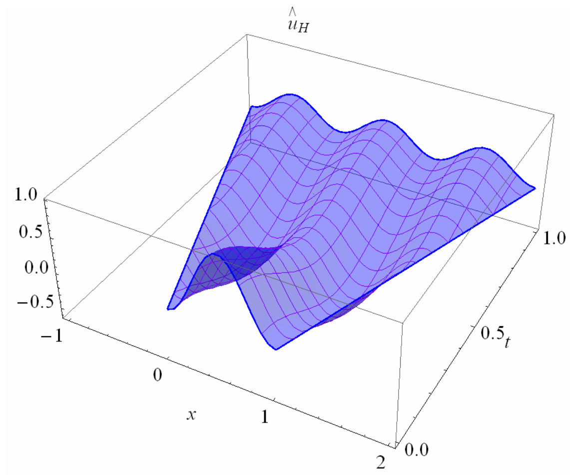

(a)

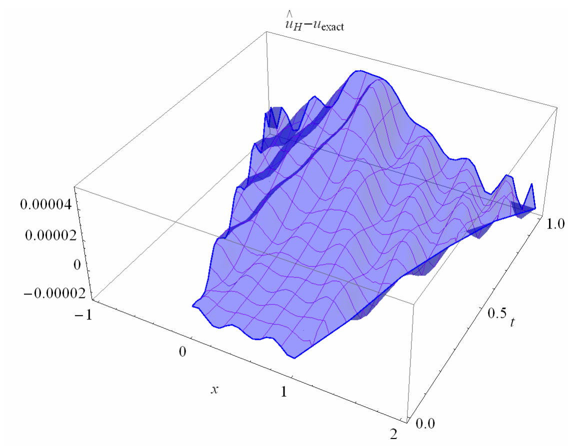

(b)

Figure 15. Variation of (a) $\hat{u}_H$, (b) $u_{exact} - \hat{u}_H$ in sample problem 7 obtained from Approach II.

8. Conclusions

We have presented a method based on using Exponential Basis Functions (EBFs) for the solution of one-dimensional time dependent problems. The EBFs are restricted to satisfy the time dependent differential equation. The solution is split into homogeneous and particular parts. The boundary and initial conditions are satisfied through a collocation method. Two approaches are introduced for satisfaction of the boundary conditions for evaluation of the homogeneous part of the solution. In one of the approaches the boundary conditions are split into homogeneous and non-homogeneous forms. The homogeneous solution with homogeneous boundary conditions is evaluated through defining a characteristic problem which has much in common with Sturm-Liouville problems; however, in this case the characteristic functions are not orthogonal necessarily and thus may not easily be used for satisfaction of the initial boundary conditions.

In another approach the homogeneous solution is evaluated without splitting the boundary conditions. The particular solution in both approaches is evaluated by the use of dual reciprocity method (DRM). In both approaches a finite time interval is used, however, with the use of such a feature we have introduced a time marching method suitable for evaluation of the complete solution over a log period of time.

We have applied the presented method to some mathematical and engineering problem. Through two mathematical problems we have shown that the two approaches are capable of solving general differential equations with constant coefficients defined in spatial coordinate and time. Five more examples are solved in the realm of engineering problem, such as heat conduction and wave propagation problems, the last two play the role of benchmarks for further studies. The results obtained in all numerical examples show the capability of the method in producing accurate results. The proposed time marching algorithm has been tested in solution of some of the examples. The results show that while the time consumed is usually less, the results are of either similar or better accuracy compared with those obtained originally. In the last example solved we have examined the capability of the method in solution of problems with moving boundaries in which we have obtained results with excellent accuracy

References

[1] G. Ruiz, HJ. Rice, An implementation of wave-based finite difference scheme for a 3-D acoustic problem, *J. Sound and Vib*., 2002, 256(2): 373-381.

[2] RJ. Astley, P. Gamallo, Special short wave elements for flow acoustics, *Comput. Methods Appl. Mech. Eng*., 2005, 194: 341–353.

[3] T. Strouboulis, R. Hidajat, I. Babuška, The generalized finite element method for Helmholtz equation. Part II: Effect of choice of handbook functions, error due to absorbing boundary conditions and its assessment, *Comput. Methods Appl. Mech. Eng*., 2008, 197: 364–380.

[4] P. Kudela, M. Krawczuk, W. Ostachowicz, Wave propagation modelling in 1D structures using spectral finite elements, *J. Sound and Vib.*, 2007, 300: 88-100.

[5] VD. Kupradze and MA. Aleksidze, The method of functional equations for the approximate solution of certain boundary value problems, *USSR Comput. Math. Math. Phys.,* 1964, 4: 82–126.

[6] G. Fairweather and A. Karageorghis, The method of fundamental solutions for elliptic boundary value problems, *Adv. Comput. Math.*, 1998, 9: 69–95.

[7] KJ. Bathe, Finite element procedures. Prentice-Hall 1996.

[8] S.Yu. Reutskiy, A Trefftz type method for time-dependent problems, *Eng. Anal. Bound. Elem.,* 2004; 28: 13-21.

[9] PM. Morse and H. Feshbach, Methods of Theoretical Physics, Part I,II, McGraw-Hill Inc. New York, 1953.

[10] FB. Hildebrand, Advanced calculus for applications, (2nd edn) Prentice-Hall Inc., New Jersey, 1976.

[11] Hokwon A. Cho, MA. Golberg, A. S. Muleshkov and Xin Li. ,Trefftz Methods for Time Dependent Partial Differential Equations, *CMC*, 2004;1 (1): 1-37.

[12] DL. Young, CC. Tsai, K. Murugesan, C.M. Fan, C.W. Chen, Time-dependent fundamental solutions for homogeneous diffusion problems, *Eng. Anal. Bound. Elem.,* 2004; 18: 1463-1473.

[13] BT. Johansson, D. Lesnic, A method of fundamental solutions for transient heat conduction, *Eng. Anal. Bound. Elem.,* 2004; 18: 1463-1473.

[14] CF. Dong, An extended method of time-dependent fundamental solutions for inhomogeneous heat conduction. *Eng. Anal. Bound. Elem.,* 2009; 33: 717-725.

[15] S. Chantasiriwan, Methods of fundamental solutions for time-dependent heat conduction problems, *Int. J. Numer. Methods Eng.,* 2006; 66: 147-165.

[16] B. Boroomand, S. Soghrati, B. Movahedian, "Exponential basis functions in solution of static and time harmonic elastic problems in a meshless style", *Int. J. Numer. Methods Eng.,* 2010; 81: 971-1018.

[17] M. Shahbazi, B. Boroomand, S. Soghrati, A mesh-free method using exponential basis functions for laminates modeled by CLPT, FSDT and TSDT; Part I: Formulation. *J. Comps. Struc.* In press. doi:10.1016/j.compstruct.2011.06.023.

[18] B. Shamsaei, B. Boroomand , Exponential Basis Functions in Solution of Laminated Structures, *J. Comps. Struc.* 2011; 93: 2010-2019.

[19] B. Boroomand, F. Mossaiby, Generalization of robustness test procedure for error estimators. Part I: formulation for patches near kinked boundaries, *Int. J. Numer. Methods Eng.,* 2005; 64: 427–60.

[20] B. Boroomand, F. Mossaiby, Generalization of robustness test procedure for error estimators. Part II: test results for error estimators using SPR and REP, *Int. J. Numer. Methods Eng.,* 2005; 64: 461–502.

[21] B. Boroomand, F. Mossaiby, Dynamic solution of unbounded domains using finite element method: Discrete Green's functions in frequency domain, *Int. J. Numer. Methods Eng*., 2006; 67: 1491–530.

[22] D. Nardini, CA. Brebbia, A new approach for free vibration analysis using boundary elements. In: Brebbia CA, editor. *Boundary element methods in engineering*. Berlin: Springer; 1982: 312–26.

[23] PW. Partridge, CA. Brebbia, LC. Wrobel, The dual reciprocity boundary element method Southampton: *Computational Mechanics*, 1992.

[24] YC. Hon, T. Wei, A fundamental solution method for inverse heat conduction problem, *Eng. Anal. Bound. Elem.,* 2004; 28: 489-495.

List of Figures

List of Tables